PLOS ONE

Cilostazol Add-On Therapy in Patients with Mild Dementia Receiving Donepezil: A Retrospective Study

Masafumi Ihara[1,2]*, Madoka Nishino[3], Akihiko Taguchi[4], Yumi Yamamoto[2], Yorito Hattori[2], Satoshi Saito[2], Yukako Takahashi[1], Masahiro Tsuji[2], Yukiko Kasahara[4], Yu Takata[3], Masahiro Okada[3]*

1 Department of Stroke and Cerebrovascular Diseases, National Cerebral and Cardiovascular Center Hospital, Osaka, Japan, **2** Department of Regenerative Medicine and Tissue Engineering, National Cerebral and Cardiovascular Center Research Institute, National Cerebral and Cardiovascular Center, Osaka, Japan, **3** Department of Neurosurgery, Sumoto Itsuki Hospital, Hyogo, Japan, **4** Department of Regenerative Medicine and Research, Institute of Biomedical Research and Innovation, Hyogo, Japan

Abstract

Goal: Combinatorial therapy directed at both vascular and neurodegenerative aspects of dementia may offer a promising strategy for treatment of dementia, which often has a multifactorial basis in the elderly. We investigated whether the phosphodiesterase III inhibitor cilostazol, which is often used in the prevention of stroke and peripheral artery disease, may delay cognitive decline in the elderly receiving donepezil.

Methods: Medical records were retrospectively surveyed to identify patients who had received donepezil for more than one year and had undergone Mini-Mental State Examination (MMSE) at least at two time points. Those with an initial MMSE score of less than 27 points were subjected to analysis (n = 156), with a cut-point of 21/22 applied to assign them to mild (n = 70) and moderate/severe (n = 86) dementia. The change of total MMSE score per year was compared between patients who had received donepezil and those given both donepezil and cilostazol.

Findings: In patients with mild dementia who had received donepezil and cilostazol (n = 34; 77.2±6.8 years old), the annual change in MMSE score was −0.5±1.6 during an observational period of 28.6±11.7 months, with those receiving donepezil only (n = 36; 78.4±6.5 years old) scoring less (−2.2±4.1) during 30.4±12.8 months with a statistical intergroup difference (p = 0.022). Multivariate analysis showed that absence of cilostazol treatment was the only significant predictor of MMSE decline. A positive effect of cilostazol was found in three subscale scores of MMSE, orientation for time or place and delayed recall. By clear contrast, in patients with moderate/severe dementia, there were no intergroup differences in decrease of total or subscale MMSE scores between the two groups.

Conclusions: These results suggest potential for cilostazol treatment in the suppression of cognitive decline in patients receiving donepezil with mild dementia but not in those with moderate/severe dementia.

Citation: Ihara M, Nishino M, Taguchi A, Yamamoto Y, Hattori Y, et al. (2014) Cilostazol Add-On Therapy in Patients with Mild Dementia Receiving Donepezil: A Retrospective Study. PLoS ONE 9(2): e89516. doi:10.1371/journal.pone.0089516

Editor: Hemachandra Reddy, Oregon Health & Science University, United States of America

Received November 9, 2013; **Accepted** January 23, 2014; **Published** February 26, 2014

Funding: This work was supported by the Takeda Visionary Research Grant from the Takeda Science Foundation (MI) and JSPS KAKENHI Grant Number 23390233 (MI). The funders had no role in study design, data collection and analysis, decision to publish, or preparation of the manuscript.

Competing Interests: The authors have declared that no competing interests exist.

* E-mail: ihara@ncvc.go.jp (MI); kmokada@sumoto.gr.jp (MO)

Introduction

Epidemiological, clinicopathological and animal studies show that vascular disease in various forms contributes to cognitive decline [1,2]. Increasing age is the strongest risk for dementia irrespective of whether it results from a vascular etiology or neurodegenerative disease processes such as in Alzheimer's disease (AD). AD and vascular cognitive impairment (VCI), the two most common causes of dementia, represent two extremes of a spectrum of disorders; however, a number of entities, which possess varying degrees of neurodegenerative and vascular pathologies, occur in between [3]. The pure forms of the disorders are preferred for convenience to label, treat or manage but conditions within the spectrum are the norm rather than the exception as dementia advances [4]. Therefore, combinatorial therapy directed at both vascular and neurodegenerative aspects of dementia may be a promising approach for the treatment of dementia in the elderly.

Cilostazol acts as an antiplatelet agent and has other pleiotropic effects based on phosphodiesterase-3-dependent mechanisms [5]. Increasing evidence suggests that cilostazol offers endothelial protection, via an inhibition of apoptosis in endothelial cells [6], attenuates the phenotypic modulation of vascular smooth muscle cells [7], and sustains blood flow by endothelium-independent vasodilation [8]. Intriguingly, cilostazol has been shown to decrease amyloid β (Aβ) accumulation and protect Aβ-induced cognitive deficits in an experimental model [9,10]. In a pilot study for 10 patients with moderate Alzheimer's disease (mean Mini-Mental Examination (MMSE) score, 11.9 points) who received donepezil, cilostazol add-on treatment for 5–6 months demonstrated significantly increased MMSE score in comparison to

baseline [11]. Moreover, cilostazol was shown to be effective in halting cognitive decline in patients with AD with cerebrovascular diseases [12] and mild cognitive impairment [13].

From the above experimental and clinical findings, we hypothesized that cilostazol has a potential to delay the cognitive decline through the pleiotropic effects in the demented elderly. We therefore retrospectively surveyed patients with dementia receiving donepezil and determined how cilostazol add-on treatment affected interval change of MMSE.

Methods

Subjects

The protocol for this study was designed in accordance with the ethical guidelines for epidemiology study established by Japan's Ministry of Education, Culture, Sports, Science and Technology in December 2008. Because this study examined only preexisting data, written informed consent was not obtained from each patient. However, we publicized the study by posting a summary of the protocol (with an easily understood description) in the Department of Neurosurgery's waiting room at Sumotoitsuki Hospital (Sumoto City, Japan); the notice clearly informed patients of their right to refuse enrolment. These procedures for informed consent and enrolment are in accordance with the detailed regulations regarding informed consent described in the guidelines, and this study, including the procedure for enrolment, has been approved by the Institutional Review Board of Sumotoitsuki Hospital. The electronic medical chart of outpatients, obtained from September 1st 1996 to June 30th 2012, was surveyed to identify cases that had history of administration of donepezil with or without cilostazol and scored MMSE at the interval of more than 1 year.

By focusing on patients whose physicians believed their clinical status was potentially ameliorated by cilostazol, we hoped to gain some degree of comparability in baseline patient characteristics between the donepezil alone and cilostazol add-on groups. To evaluate atrophy of the hippocampus, Z-scores of the voxel-based specific regional analysis system for Alzheimer's disease (VSRAD) were calculated in patients who had magnetic resonance imaging within 30 days of their initial MMSE evaluation [14]. MMSE score was evaluated mainly for purposes of applying for nursing insurance and was not necessarily linked to the date of cilostazol intake.

MMSE was scored by a single examiner who was blind to medication details. Patients who had taken cilostazol for at least 6 months during the intervals of MMSE were enrolled in the cilostazol-treated group. When MMSE was scored more than twice, the first and the last scores were selected. First, change ratio of MMSE score (point/year) was calculated according to (change in MMSE score)/([days of interval of MMSE]/365), as intervals of MMSE significantly varied between patients. Second, enrolled patients were sub-grouped based on the initial score of MMSE. Patients with an MMSE score of 22–26 were defined as mild dementia and less than 21 were moderate/severe dementia. Third, the change in each domain of MMSE score was analyzed to identify the effect of cilostazol *per se*. Hypertension, hyperlipidemia, and diabetes mellitus were defined based on the need for oral anti-hypertensive, anti-hyperlipidemic, or anti-diabetic drug therapy (or insulin), respectively, prescribed by the physician. The intake of drugs that might influence cognitive function such as angiotensin converting-enzyme inhibitor, angiotensin receptor blocker and statin (3-hydroxy-3-methylglutaryl coenzyme A reductase inhibitor) was surveyed in enrolled patients.

Statistical analysis

For statistical analysis, JMP version 9J was used. Individual comparisons were performed using a chi-square test or 2-tailed, unpaired Student's t-test. Multivariate analysis was performed to determine the effects of several variables such as age, gender, vascular risk factors and medications, including cilostazol, on the

Table 1. Comparisons of clinical profile and changes in MMSE scores in patients with moderate/severe dementia receiving donepezil (donepezil group) and donepezil plus cilostazol (combination group).

	Donepezil	Combination (donepezil/cilostazol)	p value
Number of subjects	51	35	
Sex (male/female)	17/34	14/21	0.53
Age (years)	78.2±10.5	79.3±5.9	0.58
Initial MMSE	16.5±4.8	15.9±4.2	0.51
Z-scores of VSRAD	2.82±1.57	3.13±1.40	0.39
Observational period (months)	30.2±11.9	25.8±10.2	0.08
Vascular risk factors			
Hypertension	9	10	0.23
Diabetes	6	2	0.34
Hyperlipidemia	4	5	0.34
Treatment, n			
Ca^{2+} blocker	6	6	0.48
ACE inhibitor	2	1	0.79
Diuretics	2	2	0.70
α and/or β blocker	1	2	0.35
ΔMMSE	−0.9±2.6	−0.7±2.8	0.72

MMSE, Mini-Mental State Examination; VSRAD, Voxel-Based Specific Regional Analysis System for Alzheimer's Disease; ACE, angiotensin-converting enzyme. ΔMMSE indicates the changes in MMSE scores [(follow up MMSE)–(initial MMSE)] per year. *p<0.05 in donepezil group vs. combination group.
doi:10.1371/journal.pone.0089516.t001

Table 2. Comparisons of clinical profile and changes in MMSE scores in patients with mild dementia receiving donepezil (donepezil group) and donepezil plus cilostazol (combination group).

	Donepezil	Combination (donepezil/cilostazol)	p value
Number of subjects	36	34	
Sex (male/female)	16/20	15/19	0.97
Age (years)	78.4±6.5	77.2±6.8	0.46
Initial MMSE	24.0±1.3	24.2±1.5	0.43
Z-scores of VSRAD	2.44±1.24	1.92±1.09	0.08
Observational period (months)	30.4±12.8	28.6±11.7	0.52
Vascular risk factors			
Hypertension	15	9	0.18
Diabetes	3	1	0.33
Hyperlipidemia	6	5	0.82
Treatment, n			
Ca^{2+} blocker	13	5	0.04
ACE inhibitor	2	1	0.59
Diuretics	5	0	0.02
α and/or β blocker	3	0	0.09
ΔMMSE	−2.2±4.1	−0.5±1.6	0.02

MMSE, Mini-Mental State Examination; VSRAD, Voxel-Based Specific Regional Analysis System for Alzheimer's Disease; ACE, angiotensin-converting enzyme. ΔMMSE indicates the changes in MMSE scores [(follow up MMSE)–(initial MMSE)] per year. *p<0.05 in donepezil group vs. combination group.
doi:10.1371/journal.pone.0089516.t002

annual change in MMSE. Mean ± standard deviation is shown unless stated otherwise. Significance was assumed at $p<0.05$.

Results

A total of 3183 patients had a history of cilostazol administration, including 1942 patients who took donepezil as an anti-dementia drug. With the inclusion criteria described above, we initially identified 51 patients with moderate/severe dementia (MMSE score less than 22) treated with donepezil alone (17 men and 34 women; mean 78.2 years old) and 35 patients treated with donepezil plus cilostazol (14 men and 21 women; mean 79.3 years old) (Table 1). The average daily dose of cilostazol was 139 mg/day. There was no significant difference between the donepezil group and the cilostazol add-on group in the initial MMSE score (16.5±4.8 vs. 15.9±4.2; $p=0.51$) but there was a trend for significance in the observational period (30.2±11.9 months vs. 25.8±10.2 months; $p=0.08$). The duration of cilostazol intake for cilostazol add-on group was 22.4±9.8 months. The annual change of MMSE was −0.9±2.6 in the donepezil group and −0.7±2.8 in the cilostazol add-on group, with no intergroup statistical difference ($p=0.72$). The annual change for all 11 subscale MMSE scores was also not significantly different between the two groups. Multivariate analysis did not show any significant predictors of MMSE decline among the following eight explanatory variables: age, gender, initial MMSE score, hypertension,

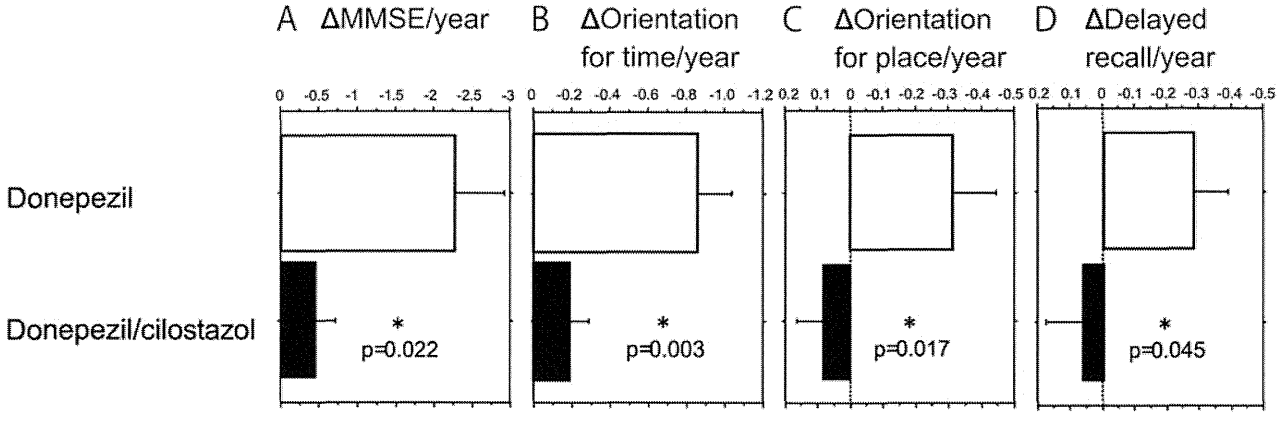

Figure 1. Cilostazol add-on therapy suppressed cognitive decline in patients with mild dementia receiving donepezil. (A) Cilostazol add-on therapy significantly suppressed decrease of total MMSE score (A) and MMSE subscale scores of orientation for time (B), orientation for place (C), and delayed recall (D) in patients with mild dementia receiving donepezil. * $p<0.05$ versus donepezil group. Error bars show standard error of the mean.
doi:10.1371/journal.pone.0089516.g001

hyperlipidemia, diabetes, cilostazol, and z score of VSRAD. Addition of other explanatory variables such as antihypertensive medications did not affect the result.

We identified a further 36 patients with mild dementia ($22 \leq$ MMSE≤ 26) treated with donepezil alone and 34 patients treated with donepezil plus cilostazol (Table 2). There were no significant differences in the initial MMSE scores (24.0 ± 1.3 vs. 24.2 ± 1.5; $p = 0.43$) or the observational period (30.4 ± 12.8 vs. 28.6 ± 11.7; $p = 0.52$) between the donepezil and the cilostazol add-on groups but there was a trend for significance in the degree of hippocampal atrophy assessed with the VSRAD when the initial MMSE was evaluated (2.44 ± 1.24 vs. 1.92 ± 1.09; $p = 0.08$). The frequency of cardiovascular risk factors including hypertension, diabetes mellitus, and hyperlipidemia was not different between the two groups but the frequency of treatment for the risk factors was significantly higher in the donepezil alone group for Ca^{2+} blockers ($p = 0.04$) and diuretics ($p = 0.02$) compared to the cilostazol add-on group. The average daily dose of cilostazol was 121 mg/day.

Intriguingly, we observed statistically significant reduced annual change in MMSE in the cilostazol add-on group compared to the donepezil group (-0.5 ± 1.6 versus -2.2 ± 4.1; $p = 0.022$) (Figure 1). Among the eight variables mentioned above, absence of cilostazol treatment was the only significant predictor of MMSE decline ($p = 0.043$). The addition of other explanatory variables, such as antihypertensive medications, did not affect the result. The annual change in MMSE subscale scores was significantly different for item 1 (orientation for time; -0.85 vs. -0.16; $p = 0.003$), item 2 (orientation for place; -0.31 vs. $+0.09$; $p = 0.017$), and item 5 (delayed recall; -0.28 vs. $+0.05$; $p = 0.045$), thus indicating a beneficial effect of cilostazol on the cognitive domains most vulnerable in AD. These results thus suggested that cilostazol suppresses cognitive decline in patients with mild dementia but not in those with established moderate/severe dementia.

Discussion

The main finding of this retrospective clinical study is that cilostazol is effective in the preservation of cognitive function for approximately two years in patients with mild dementia receiving donepezil. Multivariate analyses confirmed that only the use of cilostazol was a significant predictor of slower cognitive decline as measured by MMSE among the explanatory variables examined. Intriguingly, the positive effect of cilostazol was found in orientation for time and place and delayed recall, the cognitive domains most vulnerable in early AD.

A large-scale, randomized clinical trial demonstrated a therapeutic effect of cilostazol in the prevention of cerebral vascular disease [15]. In addition to such effects on cerebral circulation, cilostazol is known to reduce accumulation of Aβ and improve brain function in an experimental model of Alzheimer's disease [10]. The experimental study was followed by a pilot study on 10 patients with moderate Alzheimer's disease in a clinical setting where cilostazol slowed the trajectory of cognitive decline when co-administered with donepezil [11]. In addition, cilostazol was found to be effective in halting cognitive decline in patients with AD with cerebrovascular diseases [12] and mild cognitive impairment [13]. In the current study, it is apparent that cerebral circulatory impairment and Aβ accumulation may coexist and vary significantly between patients. However, this situation may be representative of that generally observed in an elderly population, indicating the clinical relevance of administering a drug that has dual roles in ischemia and Aβ-induced neurodegeneration. Thus, the preservation of cognitive function in patients with mild dementia treated with the cilostazol/donepezil combinatorial therapy may represent a finding of important clinical significance.

One of the plausible mechanistic explanations for the positive effect of combinatorial therapy is that donepezil and cilostazol have different vascular targets. Donepezil increases the level of acetylcholine, which in turn dilates vessels in an endothelium-dependent manner, while cilostazol targets PDE3 in the vascular smooth muscle cells and thus causes vasodilation in an endothelium-independent manner. We previously performed preliminary experiments using cerebrovascular β-amyloidosis mice overexpressing mutant human amyloid precursor proteins. Topical treatment with acetylcholine/cilostazol on the brain surface showed a significant increase in the vasodilatory response than that with acetylcholine alone, suggesting that cilostazol restores cerebral hemodynamic reserve in the β-amyloidosis mice (unpublished data). Several 'single-target, single-action' treatments for AD, such as anti-amyloid agents, antioxidants, and anti-inflammatory drugs, have mostly failed or performed poorly in large clinical trials [16], leading to the complementary 'neurovascular hypothesis' [17]. Multiple pathogenic cascades originating from altered vasculature can initiate disintegration of the neurovascular unit, which can amplify Aβ deposition, synaptic, neuronal and/or glial dysfunction, and subsequent cognitive decline in AD [18]. The current study therefore suggests that the vasoactive cilostazol may be a promising new therapeutic approach to maximize the potential to improve cognitive function in mildly demented patients receiving donepezil.

There are limitations to our retrospective study. First, patients with mild dementia who received cilostazol with donepezil showed a nonsignificant tendency of milder hippocampal atrophy, implying lighter neurodegenerative and heavier ischemic burden despite comparable initial MMSE score in the combinatorial therapy group. In other words, there may have been an intergroup difference in the patient demographics as a result of patient selection bias. The reasons why some patients but not others received cilostazol were unclear, which is an inherent limitation of such retrospective analyses. Second, the three major cardiovascular risk factors were more frequent in donepezil group compared to the cilostazol add-on group. This suggests an intergroup difference in background factors; however, a higher frequency of cardiovascular risk factors in the donepezil alone group may suggest a heavier ischemic burden in this group, a trend opposite to that mentioned in the first limitation. Third, we only evaluated cognitive function based on the MMSE, where multidimensional tests would have been preferable in order to evaluate cognitive function more accurately. Therefore, diagnosis of the clinical status of enrolled patients may not be sufficiently specific to allow conclusions regarding specific types of dementia. Finally, the sample size of this study is rather small; thus, comprehensive testing with a larger sample is required.

Regardless of such limitations, our results show that cognitive function can be maintained, even in a heterogeneous population with mild dementia, with cilostazol, affecting both cerebral circulation and Aβ metabolism. Since there is no fundamental treatment for dementia, development of preventive therapy is eagerly awaited. Our results highlight the need for a comprehensive prospective cohort study to analyze the effect of cilostazol on the preservation of cognitive function in patients with early-stage cognitive impairment.

Acknowledgments

We are very grateful to Dr Ahmad Khundakar for editing of this manuscript, and to Ms Noriko Kakuta for her secretarial work.

Author Contributions

Conceived and designed the experiments: MI AT MT MO. Performed the experiments: MI MN SS Y. Takahashi TK Y. Takata. Analyzed the data: YK YY YH. Contributed reagents/materials/analysis tools: MI YK YH. Wrote the paper: MI AT MO.

References

1. Gorelick PB, Scuteri A, Black SE, Decarli C, Greenberg SM, et al. (2011) Vascular contributions to cognitive impairment and dementia: a statement for healthcare professionals from the American Heart Association/American Stroke Association. Stroke 42: 2672–2713.
2. Toledo JB, Arnold SE, Raible K, Brettschneider J, Xie SX, et al. (2013) Contribution of cerebrovascular disease in autopsy confirmed neurodegenerative disease cases in the National Alzheimer's Coordinating Centre. Brain 136: 2697–2706.
3. Kalaria RN, Akinyemi R, Ihara M (2012) Does vascular pathology contribute to Alzheimer changes? J Neurol Sci 322: 141–147.
4. Kalaria RN, Ihara M (2013) Dementia: Vascular and neurodegenerative pathways-will they meet? Nat Rev Neurol. 487–488.
5. Liu Y, Shakur Y, Yoshitake M, Kambayashi JJ (2001) Cilostazol (pletal): a dual inhibitor of cyclic nucleotide phosphodiesterase type 3 and adenosine uptake. Cardiovasc Drug Rev 19: 369–386.
6. Kim KY, Shin HK, Choi JM, Hong KW (2002) Inhibition of lipopolysaccharide-induced apoptosis by cilostazol in human umbilical vein endothelial cells. J Pharmacol Exp Ther 300: 709–715.
7. Fujita Y, Lin JX, Takahashi R, Tomimoto H (2008) Cilostazol alleviates cerebral small-vessel pathology and white-matter lesions in stroke-prone spontaneously hypertensive rats. Brain Res 1203: 170–176.
8. Tanaka K, Gotoh F, Fukuuchi Y, Amano T, Uematsu D, et al. (1989) Effects of a selective inhibitor of cyclic AMP phosphodiesterase on the pial microcirculation in feline cerebral ischemia. Stroke 20: 668–673.
9. Hiramatsu M, Takiguchi O, Nishiyama A, Mori H (2010) Cilostazol prevents amyloid β peptide(25–35)-induced memory impairment and oxidative stress in mice. Br J Pharmacol 161: 1899–1912.
10. Park SH, Kim JH, Bae SS, Hong KW, Lee D-S, et al. (2011) Protective effect of the phosphodiesterase III inhibitor cilostazol on amyloid β-induced cognitive deficits associated with decreased amyloid β accumulation. Biochem Biophys Res Commun 408: 602–608.
11. Arai H, Takahashi T (2009) A combination therapy of donepezil and cilostazol for patients with moderate Alzheimer disease: pilot follow-up study. Am J Geriatr Psychiatry 17: 353–354.
12. Sakurai H, Hanyu H, Sato T, Kume K, Hirao K, et al. (2013) Effects of cilostazol on cognition and regional cerebral blood flow in patients with Alzheimer's disease and cerebrovascular disease: a pilot study. Geriatr Gerontol Int 13: 90–97.
13. Taguchi A, Takata Y, Ihara M, Kasahara Y, Tsuji M, et al. (2013) Cilostazol improves cognitive function in patients with mild cognitive impairment: A retrospective analysis. Psychogeriatrics 13: 164–169.
14. Kamiyama K, Wada A, Sugihara M, Kurioka S, Hayashi K, et al. (2010) Potential hippocampal region atrophy in diabetes mellitus type 2: a voxel-based morphometry VSRAD study. Jpn J Radiol 28: 266–272.
15. Shinohara Y, Katayama Y, Uchiyama S, Yamaguchi T, Handa S, et al. (2010) Cilostazol for prevention of secondary stroke (CSPS 2): an aspirin-controlled, double-blind, randomised non-inferiority trial. Lancet Neurol 9: 959–968.
16. Zlokovic BV (2011) Neurovascular pathways to neurodegeneration in Alzheimer's disease and other disorders. Nat Rev Neurosci 12: 723–738.
17. Chow N, Bell RD, Deane R, Streb JW, Chen J, et al. (2007) Serum response factor and myocardin mediate arterial hypercontractility and cerebral blood flow dysregulation in Alzheimer's phenotype. Proc Natl Acad Sci U S A 104: 823–828.
18. Weller RO, Djuanda E, Yow HY, Carare RO (2009) Lymphatic drainage of the brain and the pathophysiology of neurological disease. Acta Neuropathol 117: 1–14.

REVIEW

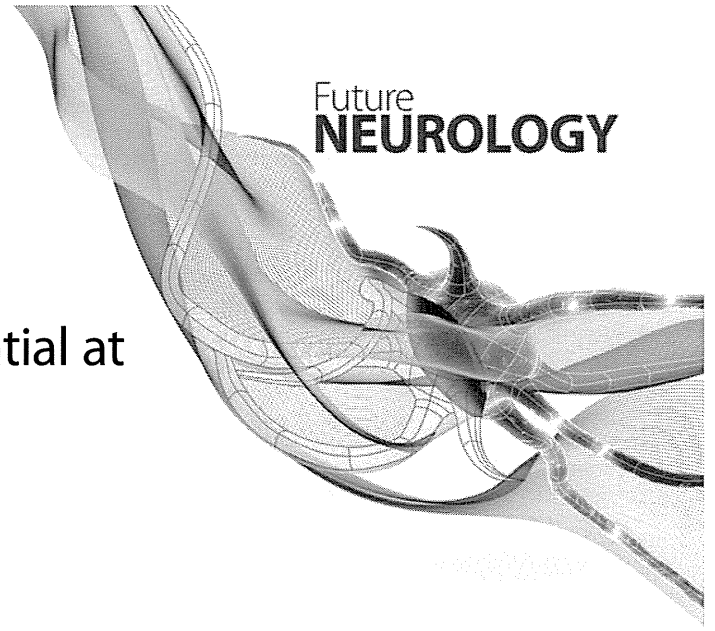

Animal models of vascular dementia: translational potential at the present time and in 2050

Hidekazu Tomimoto*[1] & Hideaki Wakita[2]

ABSTRACT: Vascular dementia is a heterogeneous syndrome, and includes subcortical ischemic vascular dementia. For translational research, subcortical ischemic vascular dementia is an appropriate target since this is the most prevalent subtype and exhibits relatively uniform clinical and neuropathological changes. These changes consist of hypertensive arteriolar changes, lacunar infarctions, hypertensive hemorrhage and white matter lesions. Among various species, rodents are most frequently used, but their small volume of white matter may impede analysis of white matter lesions. Primate models have a larger volume, but the degree of white matter lesions is inconsistent. Animal models should accommodate the effect of aging and comorbidities, and in the case of primate models, low accessibility should be overcome by repeated and quantitative examinations using modern neuroimaging techniques and functional measures, especially for memory and motor function. There is no model that replicates all features of subcortical ischemic vascular dementia and, therefore, rodent and primate models should be selected appropriately for translational research.

KEYWORDS
• Alzheimer's disease
• lacunar infarction
• subcortical ischemic vascular dementia • white matter lesions

Vascular dementia is a heterogeneous syndrome, mainly consisting of small-vessel disease with dementia, multi-infarct dementia (MID) and strategic single infarct dementia. For translational research of vascular dementia, homogeneity of disease conditions is pivotal. This is because primary outcome, including cognitive status and activity of daily living, is dependent on strategic distribution and the size of vascular lesions. Small-vessel disease is the most prevalent form of vascular dementia, with a relatively uniform clinical profile and symptoms [1]. Most patients with small-vessel disease with dementia exhibit clinical features of subcortical ischemic vascular dementia (SIVD), being consisted of multiple lacunar infarction and Binswanger's disease.

Small vessels encompass various sizes ranging from the small artery to the postcapillary venule. Among these, capillaries are the site of energy and metabolite exchange, being consisted of endothelial cells, basal lamina, pericytes and astroglial foot processes. They constitute the neurovascular unit, which is in support for the function and maintenance of neurons, and are deeply involved in the autoregulation, immune surveillance, trophic support and the maintenance of blood–brain barrier (BBB) function and hemostatic balance. With advancing ages, cerebral blood flow (CBF) decreases owing to arteriosclerosis and, therefore, the neurovascular unit is exposed to micromiliew changes due to chronic cerebral hypoperfusion, which may subsequently induce white matter lesions, upregulation of β-secretase activity and aggregation of amyloid-β (Aβ). Deposition of Aβ may in turn enhance endothelin-1 activity and vasoconstriction and disintegrate BBB, resulting in a vicious cycle between vascular insufficiency and neurodegeneration.

[1]Department of Neurology, Mie University Graduate School of Medicine, Edobashi 2-174, Tsu City 514-8507, Japan
[2]Department of Internal Medicine, Nanakuri Sanatorium, Fujita Health University, Otoricho 424-1, Tsu City 514-12957, Japan
*Author for correspondence: Tel.: +81 59 231 5107; Fax: +81 59 231 5082; tomimoto@clin.medic.mie-u.ac.jp

Future Medicine part of fsg

In 2000, the diagnostic criteria for SIVD have been proposed by Erkinjuntti *et al.* on the basis of neurological and radiological findings [2]. Radiologically, lacunar infarctions are scattered in the perforator territory, and may be accompanied by confluent white matter lesions, enlarged perivascular space, microbleeds and brain atrophy. Patients with SIVD demonstrate gradually progressive course with a relatively uniform clinical features. Therefore, SIVD is considered to be a good target of translational research for vascular dementia. The conditions necessary for recapitulating SIVD are as follows:

- Small-vessel disease includes arteriolar changes with collagen proliferation, degeneration of smooth muscle cells and narrowing of the lumen, as well as parenchymal changes with lacunar infarctions and white matter lesions;
- Large cortical infarction is basically absent in SIVD patients and, therefore, the model should not show large focal infarctions;
- Associated conditions include BBB disintegration, chronic cerebral hypoperfusion, a decrease in vasomotor reactivity and impaired cholinergic neurotransmission;
- Expression of target molecules can be manipulated either by drug administration or genetic manipulation;
- Cognitive function can be evaluated accurately and repeatedly;
- To assess a large of number of animals, inexpensive and easily accessible species are preferable;
- The primate model is superior to nonprimate models for psychological testing, although it is not easily accessible.

In this review, stroke models in which focal ischemic lesions are the major target have not been included, even though these animal models with cognitive dysfunction may simulate MID or post-stroke dementia.

Animal models for stroke & vascular dementia

Vascular dementia is causally related to stroke. Therefore, a model of stroke with cognitive and behavioral changes may be applicable to studies for vascular dementia. The effect of stroke on cognition has been extensively reviewed in a recent review [3], and is not referred to this in detail in this article. The effect of hypertension has been extensively studied in the spontaneously hypertensive rat (SHR), which develops spontaneous hypertension (**Figure 1**). SHRs were originally bred from Wistar Kyoto rats as a control strain. The SHR-stroke prone (SHR-SP) strain was further obtained by selective breeding of the SHR for stroke phenotype. SHR-SP develops hypertension with systolic blood pressure greater than 220 mmHg by 20 weeks in males and 25–30 weeks in females [4].

SHR-SP is attributed to a polygenic effect on blood pressure and is associated with overactivity of the renin–angiotensin system [5]. SHR-SP is considered to be a suitable model for studying the pathophysiology of stroke since hypertension induces arteriolar changes, such as fibrinoid degeneration and BBB disintegration [6,7]. Numerous data have been accumulated for SHR-SP, including small-vessel pathologies in concert with hemorrhage, microinfarction and white matter rarefaction [8], cerebral hypoperfusion [9] and cholinergic deficits. Cognitive impairment is also observed in SHR-SP [10–12], and occurs in the pre-stroke stage. Some of the histological lesions correspond to T2 hyperintensity in magnetic resonance images [13]. Therefore, SHR-SP is a candidate for a model of vascular dementia.

Our research group examined temporal profiles of white matter lesions in SHR-SP, and found that these lesions developed insidiously at 5–6 months of age and were mild with great variability [14]. Unfortunately, small-vessel lesions develop late in the absence of salt load, when the animals are 5–6 months of age. These temporal profiles of white mater lesions are time consuming for interventional studies and not ideal as a surrogate marker in translational research [15].

Animal models for recapitulating cardinal features of SIVD

Over the past 40 years, animal models for vascular dementia have been investigated for translational research [16]. Most of these models aimed to reproduce each feature of SIVD, encompassing lacunar infarction and white matter lesions. White matter is susceptible to cerebral ischemia because oligodendroglia, myelin-producing cells in the CNS, are sensitive to ischemic damage [17] and CNS myelin is a source of oxygen radicals during ischemia reperfusion. Indeed, hypoxia and chronic cerebral ischemia have been implicated in the pathogenesis of white matter lesions [18]. Therefore, animal models

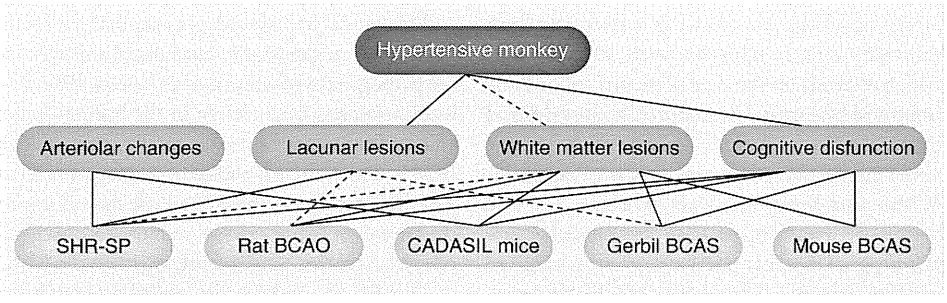

Figure 1. Neuropathological and behavioral changes in gerbil, rat, mouse and monkey models for vascular dementia. Continuous lines indicate observable findings and dashed lines indicate equivocal findings in each model.
BCAO: Bilateral carotid artery occlusion; BCAS: Bilateral carotid artery stenosis; CADASIL: Cerebral autosomal-dominant arteriopathy with subcortical infarcts and leukoencephalopathy; SHR-SP: Spontaneously hypertensive rat-stroke prone.

with white matter lesions may be achieved by chronic cerebral hypoperfusion.

• Gerbil models

Gerbils have a poorly developed posterior communicating artery and have been intensively used as an acute stroke model. Temporary occlusion of the bilateral common carotid arteries (CCAs) induces delayed neuronal death in the hippocampus, but occlusion for an extended period inevitably causes extensive brain damage and death. However, after stenosing bilateral CCAs with microcoils, gerbils show a decrease in CBF by 70–80%, and cognitive dysfunction [19] and white matter lesions by 12 weeks after chronic cerebral hypoperfusion [20]. Small necrotic foci of neuronal loss and astrogliosis are scattered in the hippocampus, basal ganglia and cerebral cortex after 1 week. Myelin basic protein and neurofilament levels are decreased, and the change in myelin basic protein precedes that of neurofilament, indicating that demyelination is the initiating pathological process [21].

• Rat models

The authors aimed to raise a rat model that forms white matter lesions by chronic cerebral hypoperfusion. This rat model of bilateral carotid artery occlusion is the most widely used model for vascular dementia. After ligation of bilateral CCAs, CBF promptly decreases to 25–52% of the baseline level in the cerebral cortices and hippocampus [22] and to 50–60% after 2 weeks [23]. White matter lesions appear latently in the periventricular area of the corpus callosum after 4 weeks of chronic cerebral hypoperfusion [24]. The optic tract and optic nerves also display a similar extent of white matter lesions, and milder lesions in the internal capsule, anterior commissure and pencil fibers in the striatum occur. There is disintegration of the BBB [25], and robust activation of microglia after 3 days and astroglia after 7 days [24]. This white matter lesion is not pure demyelination, but also accompanies axonal damage at a peak of 7–14 days in the corresponding white matter [26]. Axonal damage has been shown in human cerebrovascular white matter lesions with immunohistochemistry for fast axonal transport of proteins, such as amyloid precursor protein (APP), chromogranin A, and synaptophysin [27]. In the gray matter, there are rare foci of tissue necrosis with spongiosis in the basal ganglia, thalamus and cerebral cortex.

This rat model of chronic cerebral hypoperfusion is easy to perform and applicable to translational research. However, this model has shortcomings, such as severe derangement of the visual pathway, which may hamper appropriate estimation of cognitive function. In contrast to the CCA, bilateral occlusion of the internal carotid arteries does not impair blood flow in the ophthalmic artery, and thereby preserves visual acuity and circadian activity rhythm [28]. However, unfortunately this modified procedure induces a mild decrease in CBF and no significant white matter lesions. On cognitive function of the bilateral carotid artery occlusion rats, previous studies have reported dysfunction in passive avoidance, the Y-maze, eight-arm radial maze tasks and the Morris Water Maze task [29–32] in parallel with a decrease in cholinergic neural transmission [33,34]. These results may be explained by the fact that rodent behavior depends on information from sensory inputs, except for the visual pathway. Another disadvantage of bilateral carotid

artery occlusion rat model is a relatively high mortality rate, ranging between 10 and 50%, which depends on the type of strains and may be improved by surgical procedures, such as delayed ligation of the opposite CCA. The mortality rate varies considerably between strains of rats, with Wistar rats being relatively resistant [35]. The degree of hippocampal injury also varies because the hippocampus is particularly vulnerable to cerebral ischemia. The severity of CBF decreases in the subacute phase and the length of the observation period may predetermine the frequency of hippocampal injury, which has been reported to be absent after 4 weeks [24], or alternatively, observed as neuronal death and astrogliosis in the CA1 subfield at 4–6 months [29,33]. A recent study reported use of ameroid constrictors, which gradually stenose bilateral CCAs, and lead to a better temporal profile of CBF [36].

• Mouse models of chronic cerebral hypoperfusion

A lack of accessibility to genetically modulated animals may hamper molecular drug development in the rat. To circumvent the disadvantages of the rat model of chronic cerebral hypoperfusion, we designed a mouse model by applying microcoils to bilateral CCAs (bilateral carotid artery stenosis; BCAS; **Figure 1**). The degree of chronic cerebral hypoperfusion depends on the internal diameter of the microcoils (Sawane Spring Co., Hamamatsu, Japan) and the threshold for gray matter damage is ≤0.16 mm. CBF is decreased by 70–90% up to 4 weeks after the operation by applying 0.18 mm microcoils in 10-week-old male C57Bl/6 mice. C57Bl/6 is a strain with the most poorly developed posterior communicating arteries among various strains [37]. Therefore, manipulation of the CCAs is most effective in C57Bl/6. This BCAS model has a mortality rate of less than 20% and selective damage to white matter and working memory, but there is no damage to the hippocampus and reference memory [38–40].

Interestingly, the BCAS model shows no atrophy of the optic nerve, probably because of preserved blood flow in the ophthalmic artery, and underscore reliable assessment of cognitive function. When postischemic survival is extended to 9 months, mice show neuronal apoptosis and atrophy in the hippocampus. In addition to impairment of working memory, there also is impairment of reference memory [41]. Delayed emergence of hippocampal injury is similar to that in the rat model [29,33].

This model has advantages that make it feasible to apply to genetically modulated animals. In the pathogenesis of white matter lesions, BBB disintegration has been shown in the human brain and is also present in the rat model [25,42]. In the BCAS model, there is robust activation of matrix metalloproteinase (MMP), which may degrade the basement membrane in endothelial and glial cells [43], and this subsequently disturbs the BBB.

This BCAS model is also useful for searching for a possible link between vascular dementia and Alzheimer's disease. An increasing body of epidemiological evidences indicate a strong relationship between these two etiologies, including vascular risk factors, such as hypertension, diabetes, dyslipidemia and adiposity in midlife enhance the risk for Alzheimer's disease, and coexistence of brain vascular lesions accelerates cognitive decline in subjects with Alzheimer's disease pathology. Moreover, heart diseases, such as, aortic/mitral valve disease, atrial fibrillation and congestive heart failure, all of which seem to precipitate chronic cerebral hypoperfusion, is also the risk for Alzheimer's disease.

In a recent review, chronic cerebral hypoperfusion has been shown to accelerate Alzheimer's disease pathology and lead to a high prevalence of mixed dementia [44]. The APP transgenic mouse shows enhanced aggregation of Aβ [45] and accelerated worsening of cognitive function [46]. Chronic cerebral hypoperfusion induces microinfarction in the cerebral cortex of the transgenic cerebral amyloid angiopathy (CAA) model mouse, which expresses human vasculotropic Swedish/Dutch/Iowa mutant APP (*Tg-SwDI* mice) [47]. This study suggests that enhanced aggregation of Aβ may disturb the microcirculation. TDP43, a protein abnormally accumulated in amyotrophic lateral sclerosis and frontotemporal lobar degeneration, is also expressed in the neuronal cytoplasm after chronic cerebral hypoperfusion [48]. This link between chronic cerebral hypoperfusion and genetic manipulation may also be investigated in the unilateral common carotid artery occlusion model, which makes it feasible to compare both hemispheres of the brain [49].

• Mouse models by genetic modulation

Notch3 Arg170Cys knockin mice display arteriopathy with typical granular osmiophilic material deposition, and develop brain histopathology, including thrombosis, microbleeds, gliosis and microinfarction, as well as motor decline [50]. Arteriopathy has a late onset at approximately

8 months, with the earliest signs of motor decline at 13 months. The *PAC-Notch3* R169C rat, which overexpresses the transgene by approximately four-fold compared with endogenous Notch3 levels, shows white matter changes. Astrogliosis occurs in the *PAC-Notch3* R169C rat by 12 months and there is degeneration of white matter bundles by 20 months. The phenotypes vary depending on the species and type of genetic manipulation (knockout, knockin and transgenic), but arteriopathy with granular osmiophilic material is invariably reproducible [51,52]. The M5 muscarinic acetylcholine receptor plays a crucial role in mediating acetylcholine-dependent dilation of cerebral blood vessels. Loss of M5 muscarinic acetylcholine receptor induces arteriopathy and cognitive deficits in mice [53]. Col4A1 mice have a large deletion in type IV procollagen A1, a component of the basement membrane, and demonstrate small-vessel changes with lacunar lesions and hemorrhage [54]. R^+/A^+ mice are double transgenic for human renin and angiotensinogen [55,56], and they show hemorrhagic or ischemic lesions after treatment with a high salt diet or the nitric oxide synthase inhibitor L-N^G-nitroarginine methyl ester. CAA is reproduced in a range of transgenic mice, some of which have the human *APP* E693Q 'Dutch' mutation gene and express preferential accumulation of Aβ in small vessels without parenchymal deposits in the brain [57].

• Nonhuman primate models

Rodent white matter volume is much smaller than gray matter volume, and differs from that of the primate in which white matter constitutes half of the total brain volume. Therefore, primates are superior to rodents for replicating human white matter lesions and cognitive disorders. Coarctation of the aorta in macaque monkeys induces hypertension, and leads to scattered microinfarctions less than 500 µm in diameter in the cerebral white and gray matter, and a progressive decline in memory function 12 months after the operation. Impairment in cognitive function is correlated with systolic and diastolic blood pressure. Diffuse white matter lesions are not seen in these monkey brains and there is no SIVD-like arteriopathy [58–60].

Application of animal models in translational research for vascular dementia

Outcome measures on the effect of intervention are important for accurate evaluation for drug development. Arteriolar changes and focal infarction are not suitable for quantitative evaluation as the former demonstrates qualitative changes and the latter demonstrates heterogeneous size and distribution. Diffuse white matter lesions are highly reproducible and easy to evaluate by histological grading [24] and immunoblotting or image analysis of immunostaining for myelin basic protein or neurofilament. Astroglia and microglia are activated after chronic cerebral hypoperfusion and their number is an indicator of the degree of ischemic insult. The number of oligodendroglia decreases latently in white matter lesions. PDGFR-α-positive oligodendroglia progenitor cells are increased after chronic cerebral hypoperfusion [61,62], and conversely, some oligodendroglia show apoptotic cell death [31,63,64]. Cyclic AMP response element-binding protein-mediated oligodendrogenesis is age-related and may decline in repair mechanisms [61].

Taken together, these findings indicate that the severity of white matter lesions can be quantitatively estimated in terms of white matter integrity and glial cell number. Moreover, cognitive function may be the final indicator for therapeutic effect.

Impairment of the BBB and microglial activation occurs in the early stage of the pathological processes, and this leads to white matter lesions. The BBB is degraded by MMP2 and, therefore, gene knockout of *MMP2* suppresses glial activation and white matter lesions [42,65]. In addition, suppression of microglia by immunosuppressants and minocycline has been shown to suppress white matter lesions [66–68]. Microglia play an important role in inflammation of the CNS, and release inflammatory mediators, such as proinflammatory cytokines and oxygen radicals. Suppression of these mediators by anti-inflammatory drugs and radical scavengers is also effective in alleviating white matter lesions [69–71]. Transplantation of monocyte–microglia lineages is effective in alleviating white matter lesions, partly because these cells accumulate in the white matter and release anti-inflammatory cytokines [72,73]. Neural progenitor cells are normally generated in the subventricular zone, from where they migrate through the rostral migratory stream to the olfactory bulb in adult rodent brain. Neurogenesisis decreased after chronic cerebral hypoperfusion, and cilostazol, a phosphodiesterase III inhibitor, activates phosphorylation of CREB protein and promotes neurogenesis [74]. Cilostazol also promotes oligodendrogenesis and alleviates white

matter dysfunction in SHR-SP and chronic cerebral hypoperfusion [15,61]. It has been used in acute stroke patients and may be applicable to translational studies. Blocking of angiotensin II receptor type (AT) 1 results in relative stimulation of AT2 and AT4. AT2 has antiproliferative and vasodilative effects, and AT4 is supportive for memory function [75]. A beneficial effect of renin–angiotensin receptor inhibitors has been shown for white matter lesions and cognitive function [76–78].

Current situation for translational potential of vascular dementia

SIVD is the most appropriate subtype of vascular dementia as a therapeutic target. The reason for this is because this type of dementia is the most frequently encountered and half of these patients show progressive, but relatively uniform, symptoms, including parkinsonism subcortical dementia, pseudobulbar palsy and mental symptoms. On the contrary, there is a great variability of symptoms depending on the location and size of vascular lesions in the other type of vascular dementia including MID and strategic single infarct dementia. In particular, MID patients preferentially exhibit cortical neurological deficits, such as apraxia, aphasia and loss of cortical sensory, motor and visuospatial function with a relative preservation of memory function.

Unfortunately, past efforts in translational studies in stroke have been unsuccessful for various reasons. The Stroke Treatment Academic Industry Roundtable has defined criteria that may help to evade translational failure [79]. There are several reasons that may explain the discrepancy between positive effects in animal experiments and no therapeutic evidence in clinical trials: first, prestroke treatment is provided in animal experiments, which is unusual in the clinical setting; second, the optimal route of drug administration; third, differences in therapeutic dosage, which may exceed the safety margin in animal experiments; fourth, differences in the dose–response relationship; fifth, differences in the proportion of white matter, which constitutes half of the brain volume in primates and becomes a source of free radicals during the postischemic period; and sixth, differences in the age of animals. Most animal experiments on vascular dementia were performed in young animals without any comorbidities. However, patients with vascular dementia are usually relatively old and have multiple comorbidities, often combined with Alzheimer's pathologies. In drug development of vascular dementia, aged animals are suitable as a vascular dementia model to avoid translational failure.

With regard to the primary end points in vascular dementia, they are presumed to be motor and cognitive function, with white matter lesions as a surrogate marker. White matter lesions are sensitively and repeatedly evaluated by magnetic resonance tensor imaging, and may be a predictor of cognitive impairment in vascular dementia.

Development of white matter considerably varies among species, and this may have a large effect on cognitive impairment. Primate models are preferable in the research of white matter lesions, but the cost and accessibility are a concern for their widespread use. Therefore, there is no model for research on vascular dementia that has easy accessibility and fulfills all features of vascular dementia. Currently, the type of the model used should be selected for the research purpose of vascular dementia.

Conclusion & future perspective

Several points are anticipated to be necessary for understanding the results of animal experiments on vascular dementia. There has been increasing attention on the link between vascular dementia and Alzheimer's disease. In Alzheimer's disease, a large proportion of patients have hypertensive small-vessel disease [80]. In addition, a high frequency of mixed pathologies has been reported in neuropathological studies, including the Nun study, the HAAS, and the Hisayama study [81–83]. Acceleration of Alzheimer's pathology may be caused by enhanced β-site APP-cleaving enzyme 1 activity and Aβ clearance in vascular insufficiency. Conversely, aggravation of CAA may lead to dysregulation of the microcirculation [44]. Interstitial fluid is drained through the perivascular space and the tunica media and adventitia depending on the so-called milking of fluid by pulsation of the arterioles [84]. Driving forces by a milking mechanism could be less effective in SIVD patients with small vessel stiffening by medial-adventitial fibrosis. Very elderly people tend to have hypertensive small-vessel disease and CAA admixed with Alzheimer's disease pathology [85]. Therefore, drug development of vascular dementia should be targeted to either pure SIVD, or alternatively, mixed dementia.

Vascular dementia and Alzheimer's disease are age-associated disorders. Vascular risk factors and commodities are closely related to vascular

dementia and also to Alzheimer's disease in middle age. Therefore, animal studies for dementia should be performed on aged animals with or without vascular risk factors. The effect of aging is underscored in hippocampal atrophy in the rodent after chronic cerebral hypoperfusion. Hypoperfusion for more than several months can induce hippocampal atrophy and reference memory disturbance, suggesting that aging may lead to phenotypic modification of results obtained in young animals [41]. Indeed, atrophy and neuronal apoptosis in the hippocampus are not uncommon in SIVD.

A major effort in animal research has been devoted to postmortem brains with histological and neurochemical evaluation. Recent advancement of neuroimaging techniques has enabled the study of microarchitecture of the brain *in vivo* [86]. In the micromileu of the neuropil, neurons are functionally coupled with microvessels and adjacent glial cells, including microglia, astroglia and oligodendroglia. This neurovascular unit constitutes the smallest unit that responds to changes in external stimuli. With the use of multiphoton laser scanning microscopy, each cellular constituent of the neurovascular unit can be observed in depth, reaching to 600–700 μm from the brain surface. The BBB is composed of endothelium with basement membranes, pericytes, glia limitans and astrocyte end feet. Chronic cerebral hypoperfusion induces activation of endothelial cells with expression of adhesion molecules, and release of nitric oxide and proinflammatory cytokines. In such circumstances, the permeability of the BBB is increased more markedly in patients with vascular dementia than in those with Alzheimer's disease. Extravasation of macromolecules may impair the neurovascular unit, and may result in an increase in the cerebral spinal fluid/plasma albumin or immunoglobulin ratio, and contrast-enhanced MRI with higher dosage of gadolinium shows white matter lesions [87]. Volumetry of white matter lesions is correlated with cognitive dysfunction, but a superior correlation has been obtained by tensor MRI. Tensor MRI may enable estimation of each fiber tract, which has a varying degree of impact on cognitive function in the future.

Small animals have easy accessibility and are suitable for genetic modulation and *in vivo* imaging for microstructure of neurovascular unit. Primate models have advantages over small animals in applicability of psychological testing and similarities of brain architecture to humans. For the future translational research in 2050, modern neuroimaging techniques should be applied to nonhuman primate including fiber tract dissection and molecular and cellular trafficking on magnetic resonance images, as well

EXECUTIVE SUMMARY

Animal model for stroke & vascular dementia

- Among subtypes of vascular dementia, subcortical ischemic vascular dementia is the most suitable target for translational research of vascular dementia. Spontaneously hypertensive rat-stroke prone is hypertension-induced and ideal for replicating clinical and neuropathological features of subcortical ischemic vascular dementia.

Animal models for recapitulating cardinal features of subcortical ischemic vascular dementia

- There are various types of animal models, ranging from mice to nonhuman primates, and from surgical to genetic manipulation. The rat bilateral carotid artery occlusion model is the most popular for studies of vascular dementia.

Application of animal models in translational research for vascular dementia

- No drugs have been successful in translational research for vascular dementia. However, there have been numerous positive results in animal models.

Current situation for translational potential of vascular dementia

- The timing and route of drug administration, and age and comorbidities of animals should be taken into account. Low accessibility of primate models may be overcome using neuroimaging with quantitative and repetitive evaluation.

Future perspectives for translational research in vascular dementia

- Application of chronic cerebral hypoperfusion to genetically targeted animals may facilitate analysis of interaction between vascular dementia and Alzheimer's disease. Modern neuroimaging in primates may further enable understanding of regional heterogeneity of white matter lesions in cognitive measures.

as molecular markers for neurodegenerative diseases on PET.

Acknowledgements

The authors would like to thank all of the members of the neuropathology unit in the Department of Neurology, Kyoto University, where most of this project was carried out, as well as M Shibata (Ise Nisseki hospital, Mie) and M Ihara (National Cardiovascular Center, Osaka) for their large contribution in raising rodent models.

Financial & competing interests disclosure

The authors have no relevant affiliations or financial involvement with any organization or entity with a financial interest in or financial conflict with the subject matter or materials discussed in the manuscript. This includes employment, consultancies, honoraria, stock ownership or options, expert testimony, grants or patents received or pending, or royalties.

No writing assistance was utilized in the production of this manuscript.

References

Papers of special note have been highlighted as:

- • of interest
- •• of considerable interest

1 Pantoni L. Cerebral small vessel disease: from pathogenesis and clinical characteristics to therapeutic challenges. *Lancet Neurol.* 9(7), 689–701 (2010).

2 Erkinjuntti T, Inzitari D, Pantoni L *et al.* Research criteria for subcortical vascular dementia in clinical trials. *J. Neural Transm. Suppl.* 59, 23–30 (2000).

3 Bink DI, Ritz K, Aronica E *et al.* Mouse models to study the effect of cardiovascular risk factors on brain structure and cognition. *J. Cereb. Blood Flow Metab.* 33(11), 1666–1684 (2013).

4 Yamori Y, Horie R, Handa H *et al.* Pathogenetic similarity of strokes in stroke-prone spontaneously hypertensive rats and humans. *Stroke* 7(1), 46–53 (1976).

•• **Highlights arteriolar changes and vascular lesions in spontaneously hypertensive rat-stroke prone and established as a model of hypertension-related human stroke.**

5 Kim S, Hosoi M, Shimamoto K *et al.* Increased production of angiotensin II in the adrenal gland of stroke-prone spontaneously hypertensive rats with malignant hypertension. *Biochem. Biophys. Res. Commun.* 178(1), 151–157 (1991).

6 Fredriksson K, Auer RN, Kalimo H *et al.* Cerebrovascular lesions in stroke-prone spontaneously hypertensive rats. *Acta Neuropathol. (Berl.)* 68, 284–294 (1985).

7 Tagami M, Nara Y, Kubota A *et al.* Ultrastructural characteristics of occluded perforating arteries in stroke-prone spontaneously hypertensive rats. *Stroke* 18(4), 733–740 (1987).

8 Ogata J, Fujishima M, Tamaki K *et al.* Stroke-prone spontaneously hypertensive rats as an experimental model of malignant hypertension. I. A light- and electron-microscopic study of the brain. *Acta Neuropathol.* 51(3), 179–184 (1980).

9 Yamori Y, Horie R. Developmental course of hypertension and regional cerebral blood flow in stroke-prone spontaneously hypertensive rats. *Stroke* 8(4), 456–461 (1977).

10 Yamaguchi M, Sugimachi K, Nakano K *et al.* Memory deficit accompanying cerebral neurodegeneration after stroke in stroke-prone spontaneously hypertensive rats (SHRSP). *Acta Neurochir. Suppl. (Wien)* 60, 200–202 (1994).

11 Togashi H, Kimura S, Matsumoto M *et al.* Cholinergic changes in the hippocampus of stroke-prone spontaneously hypertensive rats. *Stroke* 27(3), 520–525 (1996).

12 Tayebati SK, Tomassoni D, Amenta F. Spontaneously hypertensive rat as a model of vascular brain disorder: microanatomy, neurochemistry and behavior. *J. Neurol. Sci.* 322(1–2), 241–249 (2012).

13 Sironi L, Guerrini U, Tremoli E *et al.* Analysis of pathological events at the onset of brain damage in stroke-prone rats: a proteomics and magnetic resonance imaging approach. *J. Neurosci. Res.* 78, 115–122 (2004b).

14 Lin JX, Tomimoto H, Akiguchi I *et al.* White matter lesions and alteration of vascular cell composition in the brain of spontaneously hypertensive rats. *Neuroreport* 12(9), 1835–1839 (2001).

15 Fujita Y, Lin JX, Takahashi R *et al.* Cilostazol alleviates cerebral small-vessel pathology and white-matter lesions in stroke-prone spontaneously hypertensive rats. *Brain Res.* 1203, 170–176 (2008).

16 Hainsworth AH, Markus HS. Do *in vivo* experimental models reflect human cerebral small vessel disease? A systematic review. *J. Cereb. Blood Flow Metab.* 28(12), 1877–1891 (2008).

• **Recent thorough review on animal models of small-vessel disease.**

17 Pantoni L, Garcia JH, Gutierrez JA. Cerebral white matter is highly vulnerable to ischemia. *Stroke* 27(9), 1641–1646 (1996).

18 Fernando MS, Simpson JE, Matthews F *et al.* White matter lesions in an unselected cohort of the elderly: molecular pathology suggests origin from chronic hypoperfusion injury. *Stroke* 37(6), 1391–1398 (2006).

19 Kudo T, Tada K, Takeda M *et al.* Learning impairment and microtubule-associated protein 2 decrease in gerbils under chronic cerebral hypoperfusion. *Stroke* 21(8), 1205–1209 (1990).

20 Hattori H, M. Takeda M, Kudo T *et al.* Cumulative white matter changes in the gerbil brain under chronic cerebral hypoperfusion. *Acta Neuropathol.* 84(4), 437–442 (1992).

21 Kurumatani T, Kudo T, Ikura Y *et al.* White matter changes in the gerbil brain under chronic cerebral hypoperfusion. *Stroke* 29(5), 1058–1062 (1998).

22 Tsuchiya M, Sako K, Yura S *et al.* Cerebral blood flow and histopathological changes following permanent bilateral carotid artery ligation in Wistar rats. *Exp. Brain Res.* 89(1), 87–92 (1992).

23 Tomimoto H, Akiguchi I, Wakita H *et al.* White matter lesions after occlusion of the bilateral carotid arteries in the rat – temporal profile of cerebral blood flow (CBF), oligodendroglia and myelin. *No To Shinkei* 49(7), 639–644 (1997).

24 Wakita H, Tomimoto H, Akiguchi I *et al.* Glial activation and white matter changes in the rat brain induced by chronic cerebral hypoperfusion: an immunohistochemical study. *Acta Neuropathol.* 87(5), 484–492 (1994).

•• **Demonstrates that chronic cerebral hypoperfusion induces white matter lesions in the rat.**

25 Ueno M, Tomimoto H, Akiguchi I *et al.* Blood–brain barrier disruption in white matter lesions in a rat model of chronic cerebral hypoperfusion. *J. Cereb. Blood Flow Metab.* 22(1), 97–104 (2002).

26 Wakita H, Tomimoto H, Akiguchi I *et al.* Axonal damage and demyelination in the white matter after chronic cerebral hypoperfusion in the rat. *Brain Res.* 924(1), 63–70 (2002).

27 Suenaga T, Ohnishi K, Nishimura M *et al.* Bundles of amyloid precursor protein-immunoreactive axons in human cerebrovascular white matter lesions. *Acta Neuropathol.* 87(5), 450–455 (1994).

28 Ohta H, Nishikawa H, Kimura H *et al.* Chronic cerebral hypoperfusion by permanent internal carotid ligation produces learning impairment without brain damage in rats. *Neuroscience* 79(4), 1039–1050 (1997).

29 Pappas BA, de la Torre JC, Davidson CM *et al.* Chronic reduction of cerebral blood flow in the adult rat: late-emerging CA1 cell loss and memory dysfunction. *Brain Res.* 708(1–2), 50–58 (1996).

30 Ulrich PT, Kroppenstedt S, Heimann A *et al.* Laser-Doppler scanning of local cerebral blood flow and reserve capacity and testing of motor and memory functions in a chronic 2-vessel occlusion model in rats. *Stroke* 29(11), 2412–2420(1998).

31 Bennett SA, Tenniswood M, Chen JH *et al.* Chronic cerebral hypoperfusion elicits neuronal apoptosis and behavioral impairment. *Neuroreport* 9(1), 161–166 (1998).

32 Sarti C, Pantoni L, Bartolini L *et al.* Cognitive impairment and chronic cerebral hypoperfusion: what can be learned from experimental models. *J. Neurol. Sci.* 203–204, 263–266 (2002).

33 Ni JW, Matsumoto K, Li HB, Murakami Y, Watanabe H. Neuronal damage and decrease of central acetylcholine level following permanent occlusion of bilateral common carotid arteries in rat. *Brain Res.* 673(2), 290–296 (1995).

34 Ouchi Y, Tsukada H, Kakiuchi T *et al.* Changes in cerebral blood flow and postsynaptic muscarinic cholinergic activity in rats with bilateral carotid artery ligation. *J. Nucl. Med.* 39(1), 198–202(1998).

35 Payan HM, Levine S, Strebel R. Effects of cerebral ischemia in various strains of rats. *Proc. Soc. Exp. Biol. Med.* 120, 208–209 (1965).

36 Kitamura A, Fujita Y, Oishi N *et al.* Selective white matter abnormalities in a novel rat model of vascular dementia. *Neurobiol. Aging* 33(5), 1012.e25–35 (2012).

37 Kitagawa K, Matsumoto M, Yang G *et al.* Cerebral ischemia after bilateral carotid artery occlusion and intraluminal suture occlusion in mice: evaluation of the patency of the posterior communicating artery. *J. Cereb. Blood Flow Metab.* 18(5), 570–579 (1998).

38 Shibata M, Ohtani R, Ihara M *et al.* White matter lesions and glial activation in a novel mouse model of chronic cerebral hypoperfusion. *Stroke* 35(11), 2598–2603 (2004).

•• **Demonstrates that chronic cerebral hypoperfusion induces white matter lesions in the mouse.**

39 Shibata M, Yamasaki N, Miyakawa T *et al.* Selective impairment of working memory in a mouse model of chronic cerebral hypoperfusion. *Stroke* 38(10), 2826–2832 (2007).

40 Ihara M, Tomimoto H. Lessons from a mouse model characterizing features of vascular cognitive impairment with white matter changes. *J. Aging Res.* 2011, 978761 (2011).

41 Nishio K, Ihara M, Yamasaki N *et al.* A mouse model characterizing features of vascular dementia with hippocampal atrophy. *Stroke* 41(6), 1278–1284 (2010).

42 Sood RR, Taheri S, Candelario-Jalil E *et al.* Early beneficial effect of matrix metalloproteinase inhibition on blood–brain barrier permeability as measured by magnetic resonance imaging countered by impaired long-term recovery after stroke in rat brain. *J. Cereb. Blood Flow Metab.* 28(2), 431–438 (2008).

43 Ihara M, Tomimoto H, Kinoshita M *et al.* Chronic cerebral hypoperfusion induces MMP-2 but not MMP-9 expression in the microglia and vascular endothelium of white matter. *J. Cereb. Blood Flow Metab.* 21(7), 828–834 (2001).

44 Iadecola C. The overlap between neurodegenerative and vascular factors in the pathogenesis of dementia. *Acta Neuropathol.* 120(3), 287–296 (2010).

45 Yamada M, Ihara M, Okamoto Y *et al.* The influence of chronic cerebral hypoperfusion on cognitive function and amyloid beta metabolism in APP overexpressing mice. *PLoS ONE* 6(1), e16567 (2011).

46 Kitaguchi, Tomimoto H, Ihara M *et al.* Chronic cerebral hypoperfusion accelerates amyloid β deposition in APPSwInd transgenic mice. *Brain Res.* 1294, 202–210 (2009).

47 Okamoto Y, Yamamoto T, Kalaria RN *et al.* Cerebral hypoperfusion accelerates cerebral amyloid angiopathy and promotes cortical microinfarcts. *Acta Neuropathol.* 123(3), 381–394 (2012).

48 Shindo A, Yata K, Sasaki R *et al.* Chronic cerebral ischemia induces redistribution and abnormal phosphorylation of transactivation-responsive DNA-binding protein-43 in mice. *Brain Res.* 1533, 131–140 (2013).

49 Yoshizaki K, Adachi K, Kataoka S *et al.* Chronic cerebral hypoperfusion induced by right unilateral common carotid artery occlusion causes delayed white matter lesions and cognitive impairment in adult mice. *Exp. Neurol.* 210(2), 585–591 (2008).

50 Wallays G, Nuyens D, Silasi-Mansat R *et al.* *Notch3* Arg170Cys knock-in mice display pathologic and clinical features of the neurovascular disorder cerebral autosomal dominant arteriopathy with subcortical infarcts and leukoencephalopathy. *Arterioscler. Thromb. Vasc. Biol.* 31(12), 2881–2888 (2011).

51 Joutel A, Monet-Leprêtre M, Gosele C *et al.* Cerebrovascular dysfunction and microcirculation rarefaction precede white matter lesions in a mouse genetic model of cerebral ischemic small vessel disease. *J. Clin. Invest.* 120(2), 433–445 (2010).

52 Joutel A. Pathogenesis of CADASIL: transgenic and knock-out mice to probe function and dysfunction of the mutated gene, *Notch3*, in the cerebrovasculature. *Bioessays* 33(1), 73–80 (2011).

53 Araya R, Noguchi T, Yuhki M *et al.* Loss of M5 muscarinic acetylcholine receptors leads to cerebrovascular and neuronal abnormalities and cognitive deficits in mice. *Neurobiol. Dis.* 24(2), 334–344 (2006).

54 Gould DB, Phalan FC, van Mil SE *et al.* Role of COL4A1 in small-vessel disease and hemorrhagic stroke. *N. Engl. J. Med.* 354(14), 1489–1496 (2006).

55 Baumbach GL, Sigmund CD, Faraci FM. Cerebral arteriolar structure in mice overexpressing human renin and angiotensinogen. *Hypertension* 41(1), 50–55 (2003).

56 Iida S, Baumbach GL, Lavoie JL *et al.* Spontaneous stroke in a genetic model of hypertension in mice. *Stroke* 36(6), 1253–1258 (2005).

57 Herzig MC, Van Nostrand WE, Jucker M. Mechanism of cerebral beta-amyloid angiopathy: murine and cellular models. *Brain Pathol.* 16(1), 40–54(2006).

58 Kemper TL, Blatt GJ, Killiany RJ *et al.* Neuropathology of progressive cognitive decline in chronically hypertensive rhesus monkeys. *Acta Neuropathol.* 101(2), 145–153 (2001).

59 Moore TL, Killiany RJ, Rosene DL *et al.* Impairment of executive function induced by hypertension in the rhesus monkey (*Macaca mulatta*). *Behav. Neurosci.* 116(3), 387–396 (2002).

60 Moss MB, Jonak E. Cerebrovascular disease and dementia: a primate model of hypertension and cognition. *Alzheimers Dement.* 3(2 Suppl.), S6–S15 (2007).

61 Miyamoto N, Pham LD, Hayakawa K *et al.* Age-related decline in oligodendrogenesis retards white matter repair in mice. *Stroke* 44(9), 2573–2578 (2013).

62 Arai K, Lo EH. An oligovascular niche: cerebral endothelial cells promote the survival and proliferation of oligodendrocyte precursor cells. *J. Neurosci.* 29(14), 4351–4355 (2009).

63 Tomimoto H, Ihara M, Wakita H *et al.* Chronic cerebral hypoperfusion induces white matter lesions and loss of oligodendroglia with DNA fragmentation in the rat. *Acta Neuropathol.* 106(6), 527–534 (2003).

64 Mandai K, Matsumoto M, Kitagawa K *et al.* Ischemic damage and subsequent proliferation of oligodendrocytes in focal cerebral ischemia. *Neuroscience* 77(3), 849–861 (1997).

65 Nakaji K, Ihara M, Takahashi C *et al.* Matrix metalloproteinase-2 plays a critical role in the pathogenesis of white matter lesions after chronic cerebral hypoperfusion in rodents. *Stroke* 37(11), 2816–2823 (2006).

66 Wakita H, Tomimoto H, Akiguchi I *et al.* Protective effect of cyclosporin A on white matter changes in the rat brain after chronic cerebral hypoperfusion. *Stroke* 26(8), 1415–1422 (1995).

67 Wakita H, Tomimoto H, Akiguchi I *et al.* Dose dependent, protective effect of FK506 against white matter changes in the rat brain after chronic cerebral ischemia. *Brain Res.* 792(1), 105–113 (1998).

68 Cho KO, La HO, Cho YJ *et al.* Minocycline attenuates white matter damage in a rat model of chronic cerebral hypoperfusion. *J. Neurosci. Res.* 83(2), 285–291 (2006).

69 Institoris A, Farkas E, Berczi S *et al.* Effects of cyclooxygenase (COX) inhibition on memory impairment and hippocampal damage in the early period of cerebral hypoperfusion in rats. *Eur. J. Pharmacol.* 574(1), 29–38 (2007).

70 Wakita H, Ruetzler C, Illoh KO *et al.* Mucosal tolerization to E-selectin protects against memory dysfunction and white matter damage in a vascular cognitive impairment model. *J. Cereb. Blood Flow Metab.* 28(2), 341–353 (2008).

71 Ueno Y, Zhang N, Miyamoto N *et al.* Edaravone attenuates white matter lesions through endothelial protection in a rat chronic hypoperfusion model. *Neuroscience* 162(2), 317–327 (2009).

72 Narantuya D, Nagai A, Sheikh AM *et al.* Microglia transplantation attenuates white matter injury in rat chronic ischemia model via matrix metalloproteinase-2 inhibition. *Brain Res.* 1316, 145–152 (2010).

73 Fujita Y, Ihara M, Ushiki T *et al.* Early protective effect of bone marrow mononuclear cells against ischemic white matter damage through augmentation of cerebral blood flow. *Stroke* 41(12), 2938–2943(2010).

74 Miyamoto N, Tanaka R, Zhang N *et al.* Crucial role for Ser133-phosphorylated form of cyclic AMP-responsive element binding protein signaling in the differentiation and survival of neural progenitors under chronic cerebral hypoperfusion. *Neuroscience* 162(2), 525–536 (2009).

75 Phillips MI, de Oliveira EM. Brain renin angiotensin in disease. *J. Mol. Med. (Berl.)* 86(6), 715–722 (2008).

76 Kumaran D, Udayabanu M, Kumar M *et al.* Involvement of angiotensin converting enzyme in cerebral hypoperfusion induced anterograde memory impairment and cholinergic dysfunction in rats. *Neuroscience* 155(3), 626–639 (2008).

77 Washida K, Ihara M, Nishio K *et al.* Nonhypotensive dose of telmisartan attenuates cognitive impairment partially due to peroxisome proliferator-activated receptor-γ activation in mice with chronic cerebral hypoperfusion. *Stroke* 41(8), 1798–1806 (2010).

78 Dong YF, Kataoka K, Toyama K *et al.* Attenuation of brain damage and cognitive impairment by direct renin inhibition in mice with chronic cerebral hypoperfusion. *Hypertension* 58(4), 635–642 (2011).

79 Stroke Therapy Academic Industry Roundtable (STAIR). Recommendations for standards regarding preclinical neuroprotective and restorative drug development. *Stroke* 30(12), 2752–2758 (1999).

80 Carotenuto A, Rea R, Colucci L *et al.* Late and early onset dementia: what is the role of vascular factors? A retrospective study. *J. Neurol. Sci.* 322(1–2), 170–175 (2012).

81 Snowdon DA, Greiner LH, Mortimer JA *et al.* Brain infarction and the clinical expression of Alzheimer disease. The Nun study. *JAMA* 277(10), 813–817 (1997).

82 Petrovitch H, Ross GW, Steinhorn SC *et al.* AD lesions and infarcts in demented and non-demented Japanese–American men. *Ann. Neurol.* 57(1), 98–103 (2005).

83 Matsui Y, Tanizaki Y, Arima H *et al.* Incidence and survival of dementia in a general population of Japanese elderly: the Hisayama study. *J. Neurol. Neurosurg. Psychiatry* 80(4), 366–370 (2009).

84 Schley D, Carare-Nnadi R, Please CP *et al.* Mechanisms to explain the reverse perivascular transport of solutes out of the brain. *J. Theor. Biol.* 238(4), 962–974 (2006).

85 Thal DR, Ghebremedhin E, Orantes M *et al.* Vascular pathology in Alzheimer disease: correlation of cerebral amyloid angiopathy and arteriosclerosis/lipohyalinosis with cognitive decline. *J. Neuropathol. Exp. Neurol.* 62(12), 1287–1301 (2003).

86 Wardlaw JM, Smith EE, Biessels GJ *et al.* Neuroimaging standards for research into small vessel disease and its contribution to ageing and neurodegeneration. *Lancet Neurol.* 12(8), 822–838 (2013).

87 Taheri S, Gasparovic C, Huisa BN *et al.* Blood–brain barrier permeability abnormalities in vascular cognitive impairment. *Stroke* 42(8), 2158–2163 (2011).

Journal of Neuroscience Methods 221 (2014) 139–150

Contents lists available at ScienceDirect

Journal of Neuroscience Methods

journal homepage: www.elsevier.com/locate/jneumeth

Clinical Neuroscience

A comparison of three brain atlases for MCI prediction

Kenichi Ota[a], Naoya Oishi[a,*], Kengo Ito[b], Hidenao Fukuyama[a], the SEAD-J Study Group[1]

[a] Human Brain Research Center, Kyoto University Graduate School of Medicine, 54 Shogoin-Kawahara-cho, Sakyo-ku, Kyoto 606-8507, Japan
[b] Clinical and Experimental Neuroimaging, National Center for Geriatrics and Gerontology, 35 Gengo, Morioka-machi, Obu-shi, Aichi 474-8511, Japan

HIGHLIGHTS

- We examine MCI classification accuracy with three atlas-based parcellation methods.
- Gray matter density differs between two groups in the left hippocampal region.
- SVM classification using the LPBA40 atlas provides the highest accuracy of 77.9%.
- SVM-RFE algorithm enhances the performance regardless of the choice of atlases.

ARTICLE INFO

Article history:
Received 7 May 2013
Received in revised form 3 October 2013
Accepted 4 October 2013

Keywords:
Alzheimer's disease (AD)
Mild cognitive impairment (MCI)
Magnetic resonance imaging (MRI)
Voxel-based morphometry (VBM)
Support vector machine (SVM)
Atlas-based parcellation

ABSTRACT

Background: Although previous voxel-based studies using features extracted by atlas-based parcellation produced relatively poor performances on the prediction of Alzheimer's disease (AD) in subjects with mild cognitive impairment (MCI), classification performance usually depends on features extracted from the original images by atlas-based parcellation. To establish whether classification performance differs depending on the choice of atlases, support vector machine (SVM)-based classification using different brain atlases was performed.
New method: Seventy-seven three-dimensional T1-weighted MRI data sets of subjects with amnestic MCI, including 39 subjects who developed AD (MCI-C) within three years and 38 who did not (MCI-NC), were used for voxel-based morphometry (VBM) analyses and analyzed using SVM-based pattern recognition methods combined with a feature selection method based on the SVM recursive feature elimination (RFE) method. Three brain atlases were used for the feature selections: the Automated Anatomical Labeling (AAL) Atlas, Brodmann's Areas (BA), and the LONI Probabilistic Brain Atlas (LPBA40).
Results: The VBM analysis showed a significant cluster of gray matter density reduction, located at the left hippocampal region, in MCI-C compared to MCI-NC. The SVM analyses with the SVM-RFE algorithm revealed that the best classification performance was achieved by LPBA40 with 37 selected features, giving an accuracy of 77.9%. The overall performance in LPBA40 was better than that of AAL and BA regardless of the number of selected features.
Conclusions: These results suggest that feature selection is crucial to improve the classification performance in atlas-based analysis and that the choice of atlases is also important.

1. Introduction

Although there is no real treatment for Alzheimer's disease (AD), medications currently available to alleviate cognitive and behavioral symptoms of AD may delay clinical progression to AD (Petersen et al., 2005). AD pathophysiological processes precede the clinical manifestation of symptoms of AD. The earlier the intervention against symptomatic progression begins, the more effective the intervention may be. Earlier diagnosis or prediction of the conversion of mild cognitive impairment (MCI) to AD is therefore required for earlier intervention. It is necessary to explore effective biomarkers for early AD detection in the earliest stages of the disease.

The recently revised diagnostic criteria for AD incorporated biomarkers of neuronal injury such as brain atrophy (Albert et al., 2011). Currently, even clinical magnetic resonance imaging (MRI) scanners allow the acquisition of images with high spatial resolution, to provide AD biomarkers that reflect brain atrophy (Frisoni

* Corresponding author. Tel.: +81 75 751 3695; fax: +81 75 751 3202.
E-mail addresses: otak@kuhp.kyoto-u.ac.jp (K. Ota), noishi@kuhp.kyoto-u.ac.jp (N. Oishi), kito@ncgg.go.jp (K. Ito), fukuyama@kuhp.kyoto-u.ac.jp (H. Fukuyama).
[1] Data used in the preparation of this article were obtained from the Research group of the Studies on Diagnosis of Early Alzheimer's Disease-Japan (SEAD-J), which comprised investigators from nine different facilities. As such, the investigators within the SEAD-J study group contributed to the design and implementation of SEAD-J and/or provided data but did not participate in the analysis or writing of this report.

0165-0270/$ – see front matter © 2013 Elsevier B.V. All rights reserved.
http://dx.doi.org/10.1016/j.jneumeth.2013.10.003

et al., 2010). Structural MRI-based features that are widely used in such pattern recognition methods include: voxel-based whole brain volume data, surface-based measures such as cortical thickness, and features based on specific regions of interest (ROIs) such as hippocampus and entorhinal cortex. In this context, MRI studies across the whole brain, such as voxel-based morphometry (VBM) techniques (Ashburner and Friston, 2000), could be more useful in investigating biomarkers for early AD detection, rather than those based on specific ROIs. For example, Karas et al. (2004) conducted a VBM study to analyze patterns of gray matter (GM) loss and revealed that subjects with MCI had significant local GM reductions in the medial temporal lobe, the insula, and the thalamus compared to normal elderly controls. GM loss on structural MRI can be shown in a specific topographic pattern involving temporal lobes and parietal cortices (Jack et al., 2011). VBM studies have also demonstrated that patterns of GM loss correlate with neurofibrillary tangle pathology (Vemuri et al., 2008; Whitwell et al., 2008). AD neuropathology is mainly characterized by the extracellular deposition of fibrillary β-amyloid protein and intracellular formation of neurofibrillary tangles composed of abnormal tau protein (Nelson et al., 2009). Braak et al. (2011) reported that β-amyloid protein and neurofibrillary tangles were significantly correlated and that pathological aggregation of tau protein might begin earlier than previously thought; these authors also suggest that possibly these events occur in subcortical nuclei rather than in the transentorhinal region of the perirhinal cortex.

Pattern recognition methods based on machine-learning techniques such as the support vector machine (SVM) are promising tools for computer-aided diagnosis of AD (Klöppel et al., 2008, 2012). It is, however, currently unrealistic to use a hundred thousand voxels of MRI data for each scan directly for machine-learning-based pattern recognition, because of the possibility of poor generalization from overfitting, which could arise in a case in which the number of features is much larger than the number of subjects. Therefore, dimensionality reduction in the feature space, such as feature extraction and feature selection, is usually necessary to achieve good generalization, which is required for possible clinical utility.

Among various approaches to classifying subjects with MCI using structural MRI, voxel-based methods can be roughly classified into two categories: data-driven adaptive feature extraction methods (Fan et al., 2007; Misra et al., 2009; Davatzikos et al., 2011) and atlas-based parcellation methods, using a predefined brain atlas (Cuingnet et al., 2011; Cho et al., 2012). Data-driven feature extraction methods adaptively define ROIs depending on the input data without a predefined brain atlas, which are difficult to interpret anatomically. On the other hand, atlas-based parcellation methods allow feature vector extraction with good anatomical interpretability. An atlas-based parcellation approach can be used as an anatomical filter for dimensionality reduction to construct gray matter volumes for dozens of predetermined ROIs from hundreds of thousands of voxels in each subject's whole-brain structural MRI. The extracted regional feature variables for each subject can be employed to create multivariate models to classify each subject into different groups (Whitwell et al., 2011). Examples of such an anatomical brain atlas include Brodmann's areas (BA; Brodmann, 1909) and the Automated Anatomical Labeling Atlas (AAL; Tzourio-Mazoyer et al., 2002). These atlases are publicly available from the Internet, in open source software packages (MRIcro/MRIcron, http://www.mricro.com/). Although previous benchmark studies showed poor classification performance of an atlas-based method (Cuingnet et al., 2011; Cho et al., 2012), classification performance strongly depends on the features that are extracted from the atlas used for parcellation. It remains unclear whether atlas-based parcellation methods applied to different atlases would in fact lead to different classification performances.

The aim of our study was to establish whether the performance when predicting conversion to AD using GM volumes from the structural MRI of subjects with MCI differs depending on the choice of the atlas. To accomplish this goal, SVM-based classification using three different brain atlases was used. We also investigated whether a feature selection method could enhance the classification accuracy.

2. Materials and methods

2.1. Subjects

Studies on the Diagnosis of Early Alzheimer's Disease—Japan (SEAD-J), a prospective multicenter cohort study of subjects with amnestic MCI was started in 2005 by the National Center for Geriatrics and Gerontology, to achieve the early prediction of AD conversion (Kawashima et al., 2012). In this cohort study, 114 subjects with amnestic MCI were recruited from nine different facilities across Japan (Supplementary Table 1) between January 2006 and March 2007. All of the subjects were living independently in the community at the time of their baseline evaluation. This study was approved by the Ethics Committee at every participating institution. Each subject signed an informed consent form after a full explanation of the procedures had been offered.

Diagnosis of MCI was based on an interview with neurologists that contained evidence of reduced cognitive capacity, normal activities of daily living, and the absence of dementia (Cui et al., 2011). All of the patients were free of significant underlying medical, neurological, or psychiatric illness. The patients were initially accessed using a neuropsychological test battery, including the Mini-Mental State Examination (MMSE; Folstein et al., 1975), Alzheimer's Disease Assessment Scale-Cognitive Subscale, Japanese version (ADAS-J cog; Homma et al., 1992), Clinical Dementia Rating (CDR; Morris, 1993), Geriatric Depression Scale (GDS; Yesavage et al., 1982; Nyunt et al., 2009), Everyday Memory Checklist (EMC; Kazui et al., 2003), and the Wechsler Memory Scale-Revised Logical memory test (WMS-R LM; Sullivan, 1996). In accordance with the inclusion criteria, MCI patients were between 50 and 80 years old, with an MMSE score ≥ 24, a GDS score ≤ 10, a WMS-R LM I score ≤ 13, an LM II part A and part B score (maximum, 50) ≤ 8, and a CDR memory box score restricted to 0.5. Patients who had an educational level (defined as the number of completed years of formal education) of under 6 years were excluded. The patients were observed at 1-year intervals for 3 years and underwent the following standardized procedures. Trained clinicians performed baseline and follow-up 1-year evaluations. The CDR, MMSE, EMC, and WMS-R-LM were completed at each visit during follow-up. ^{18}F-2-fluoro-2-deoxy-D-glucose (FDG) positron emission tomography (PET) and MRI were optional during follow-up. The ADAS-J cog was also administered as an option in selected centers. Conversion to dementia was established when CDR became ≥ 1. The diagnosis of AD was made in a given center if a patient fulfilled both CDR ≥ 1 and the National Institute of Neurological Disorders and Stroke–Alzheimer's Disease and Related Disorders Association (NINCDS-ADRDA) probable AD criteria (McKhann et al., 1984). The diagnosis of other causes was based on established clinical criteria for each disease, including vascular dementia (VaD) (Devanand et al., 2010), dementia with Lewy bodies (DLB) (McKeith et al., 1996), frontotemporal dementia (FTD) (McKhann et al., 2001), and Creutzfeldt-Jakob disease (CJD) (Knopman et al., 2001).

Of all of the 114 participants, 37 subjects were excluded from our analyses due to the following reasons: 2 had no baseline three-dimensional T1-weighted MRI scans, 3 converted to non-AD

Table 1
Demographic and neuropsychological data of MCI-C and MCI-NC subjects at baseline.

	MCI-C ($n=39$)	MCI-NC ($n=38$)	p-value
Age [years]	71.3 ± 6.7	70.6 ± 6.9	0.65
Female/Male	20/19	22/16	0.32
Education [years]	12.2 ± 3.2	11.8 ± 3.1	0.62
WMS-R LM I (immediate recall)	6.5 ± 3.3	9.4 ± 3.1	$<10^{-3}$*
WMS-R LM II (delayed recall)	1.6 ± 2.2	4.3 ± 2.9	$<10^{-4}$*
MMSE	25.6 ± 1.8	27.0 ± 2.0	0.003*
ADAS-J cog	9.9 ± 4.7	7.8 ± 4.6	0.046*
GDS	4.9 ± 2.3	3.4 ± 1.8	0.004*

MCI-C, MCI converters; MCI-NC, MCI non-converters; WMS-R LM, Wechsler Memory Scale-Revised Logical memory; MMSE, Mini-Mental State Examination; ADAS-J cog, Alzheimer's Disease Assessment Scale-Cognitive Subscale, Japanese version; GDS, Geriatric Depression Scale.
Age, education, and neuropsychological test scores are shown with mean ± SD.
* t-Test, $p<0.05$.

dementia (VaD, DLB, and FTD), 23 withdrew from the study within 3 years, and 9 were excluded due to the lack of whole-brain coverage in their baseline T1-weighted MRI scans.

As a result, we identified 77 subjects with amnestic MCI from the SEAD-J comprising 39 who developed AD within 3 years (AD converters, MCI-C; 20 females, 19 males; age ± SD = 71.3 ± 6.7 years ranging from 50 to 79 years; and MMSE = 25.6 ± 1.8 ranging from 24 to 30) and 38 who did not (non-converters, MCI-NC; 22 females, 16 males; age ± SD = 70.6 ± 6.9 years ranging from 55 to 79 years; and MMSE = 27.0 ± 2.0 ranging from 24 to 30). Among these AD converters, 21 converted to AD within 1 year after inclusion, 14 within 2 years, and 4 within 3 years. Baseline demographic data and neuropsychological test results of these subjects are shown in Table 1. The two groups significantly differed in the MMSE, ADAS-J cog, WMS-R-LM, and GDS scores at the baseline. No significant differences were observed in the age, gender, and education.

2.2. MRI acquisition and preprocessing

A three-dimensional structural MRI at the baseline was acquired on each subject with T1-weighted gradient echo sequences on 1.5 T or 3.0 T MRI scanners at the nine facilities. Details about MRI acquisition conditions are provided in Supplementary Table 2.

We used the SPM8 (http://www.fil.ion.ucl.ac.uk/spm/software/spm8) and VBM8 Toolbox (Kurth et al., 2010; http://dbm.neuro.uni-jena.de/vbm) on MATLAB 7.12 for preprocessing the baseline MRI data. The images were first segmented into GM, white matter and cerebrospinal fluid using Unified Segmentation (Ashburner and Friston, 2005) implemented in SPM8 and a technique based on the maximum a posteriori (MAP) estimation (Rajapakse et al., 1997) and the Partial Volume Estimation (PVE) (Tohka et al., 2004) implemented in VBM8 with standard parameters. Then, the segmented images were spatially normalized using the Diffeomorphic Anatomical Registration using the Exponentiated Lie algebra (DARTEL) algorithm (Ashburner, 2007). Jacobian modulation was applied to compensate for the effect of spatial normalization and to restore the original absolute GM density in the segmented GM images. The normalized, segmented, and modulated images were smoothed with an 8-mm full-width at half-maximum isotropic Gaussian kernel.

2.3. Voxel-based morphometry (VBM) analysis

The smoothed baseline MR images were analyzed using a conventional VBM method (Ashburner and Friston, 2000) to investigate the differences in the density of the GM between the MCI-C and the MCI-NC group. We conducted a statistical analysis that included an adjustment for age, gender, and scan facilities as covariates using SPM8. The statistical threshold was set at $p<0.001$, was uncorrected for multiple comparisons and was cluster-level corrected for multiple comparisons ($p<0.05$).

2.4. Feature extraction using atlas-based parcellation

We performed atlas-based parcellation to extract feature vectors from the segmented, normalized MR images using three different anatomically labeled brain atlases: the AAL atlas, BA, and the LONI Probabilistic Brain Atlas (LPBA40; Shattuck et al., 2008) (Fig. 1).

The AAL atlas is a single-subject atlas based on the Montreal Neurological Institute (MNI) Colin27 T1 atlas. This MNI single-subject brain template was obtained from 27 high-resolution T1-weighted scans of a young male. Each acquisition was spatially normalized to the MNI305 average template using a linear nine-parameter transformation (Holmes et al., 1998). In each hemisphere, 45 ROIs were drawn manually every 2 mm on the axial slices of the MNI single-subject brain. In addition, AAL includes a cerebellar parcellation with 26 ROIs (Schmahmann et al., 1999, 2000) (Fig. 1). Finally, 116 ROIs were defined, including the cerebellum for the AAL atlas.

The BA of the human cortex originally shows 43 cytoarchitectonic areas (Brodmann, 1909), where areas with the numbers 12–16 and 48–51 are not shown (Zilles and Amunts, 2010). We used the BA atlas in MRIcro with 41 areas, where BA 31 (dorsal posterior cingulate area), 33 (pregenual area), and 52 (parainsular area) were not included, and BA 48 (retrosubicular area) was included. For the purpose of the comparison with the other two atlases, we subdivided each of the 41 areas of BA symmetrically with respect to the mid-sagittal plane to obtain 82 ROIs in total (Fig. 1). Both AAL and BA in MRIcro were based on the "ch2" image, which was created using 27 scans from a single individual (Holmes et al., 1998).

The LPBA40 atlas is a population-based probabilistic atlas that is constructed from high-resolution T1-weighted MRI scans of 40 healthy, normal volunteers comprising 20 males and 20 females with the average age of 29.2 ± 6.3 years (mean ± SD; min = 19.3, max = 39.5) (Shattuck et al., 2008). LPBA40 has three variants depending on the spatial normalization strategy. We used the LPBA40/AIR version. Each of the 40 volumes was aligned to the ICBM 452 T1 Warp 5 Atlas (ICBM452W5). The ICBM452W5 was created from 452 brains, and each volume was normalized to MNI305 average brains using a linear 12-parameter transformation and a subsequent non-linear 5th-order polynomial warping. In LPBA40, a total of 56 structures were manually labeled, including 50 cortical structures, 4 subcortical nuclei, the brainstem, and the cerebellum (Fig. 1).

We obtained deformation fields in the same manner as the above spatial normalization. Then we applied the forward deformation field to each atlas ROIs to map to MNI space. The mean GM density within each ROI, as calculated by modulation with the Jacobian, was computed with linear regression to adjust image quality differences among the facilities and used as the feature vectors.

2.5. Classification using a support vector machine (SVM)

Multivariate pattern recognition analysis using machine-learning methods has been applied to the classification of MCI subjects. In particular, SVM (Vapnik, 1998) is one of the widely used methods because of its remarkable performance of classification as well as the simplicity of its theory and implementation. For example, Aguilar et al. (2013) demonstrated that SVM was superior to other multivariate classifiers for classification of subjects with AD and cognitive normal and SVM also provided similar predictive values for MCI differentiation although there were no significant differences between classifiers. Accordingly,

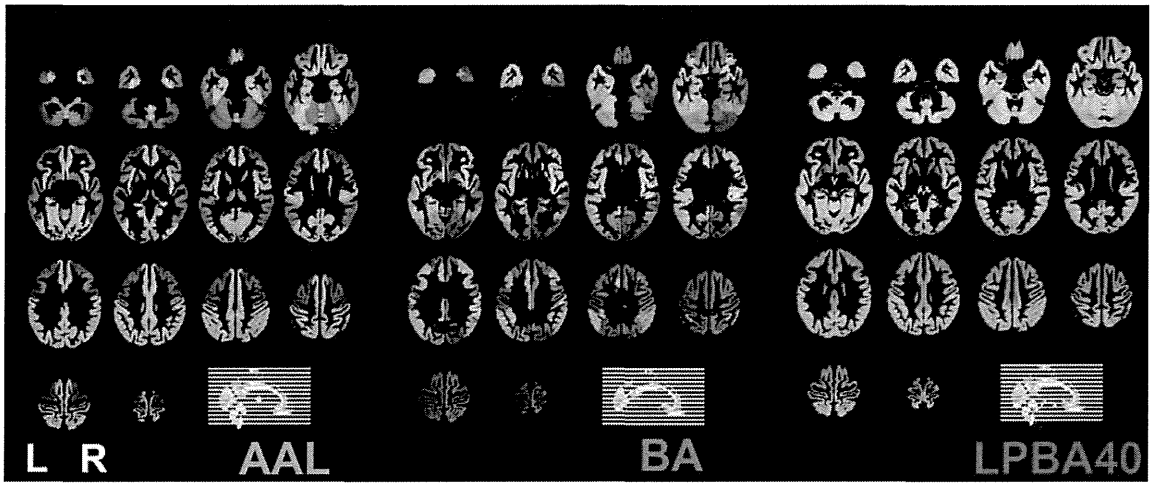

Fig. 1. Three brain atlases used for feature extraction, overlaid to representative structural MR images. AAL, Automated Anatomical Labeling; BA, Brodmann's areas; LPBA40, LONI Probabilistic Brain Atlas.

we chose SVM as a classifier for predicting the conversion from MCI to AD because we anticipated achieving a better classification performance.

We used an SVM classifier with a radial basis function (RBF) in accordance with the practical guide by Hsu et al. (2003). The classification performance was assessed using a leave-one-out cross-validation (LOOCV) strategy. We used MATLAB 7.6 and the LIBSVM library (Chang and Lin, 2011; Software available at http://www.csie.ntu.edu.tw/~cjlin/libsvm) to implement an RBF-kernel SVM with LOOCV. The hyperparameters (C, γ) of the RBF kernel were optimized using a two-step grid-search technique with 5-fold cross-validation according to the recommendation described in a practical guide to SVM classification (Hsu et al., 2003). First, the best pair of C_{coarse} and γ_{coarse} was found by a coarse grid-search on $\log_2 C = -5, -3, \ldots, 15$ and $\log_2 \gamma = -15, -13, \ldots, 3$. Then, the best pair of C_{fine} and γ_{fine} was obtained by a fine grid-search on $\log_2 C = C_{coarse} - 2, C_{coarse} - 1.75, \ldots, C_{coarse} + 1.75, C_{coarse} + 2$ and $\log_2 \gamma = \gamma_{coarse} - 2, \gamma_{coarse} - 1.75, \ldots, \gamma_{coarse} + 1.75, \gamma_{coarse} + 2$. The best ($C_{fine}$, γ_{fine}) was used to generate the final classifier for each training set.

2.6. Feature selection using the SVM recursive feature elimination (SVM-RFE)

In general, feature sets that are extracted from an input data set still contain redundant or irrelevant features as well as those that are important for classification. The higher the dimension the feature space is, the worse the performance of the classification. The ultimate goal of pattern recognition is to improve the generalization.

To enhance the performance of SVM-based classification, we performed a feature selection method that was based on the support vector machine recursive feature elimination (SVM-RFE) algorithm (Guyon et al., 2002). The SVM-RFE algorithm uses SVM to produce a feature ranking. Features that do not contribute to separation are eliminated according to the feature ranking. We used a linear kernel in the SVM-RFE procedure in the same manner as the original algorithm proposed by Guyon et al. (2002), and implemented the algorithm using MATLAB 7.6 according to the literature (Guyon et al., 2002). The hyperparameter C of the linear kernel was optimized using a two-step grid-search technique with 5-fold cross-validation in a similar manner to the above. A total of 77 feature ranked lists were obtained by the following SVM-RFE LOOCV iterative process:

```
Inputs: feature vectors X0 = [x1, x2, ..., xi, xn]^T and class labels y = [y1,
  y2, ..., yi, ..., yn]^T
for i = 1 to n
  Split X0 into a test set (subject i) and a training set (the remaining subjects)
  Initialize:
  Subset of surviving features: s = [1,2, ..., m]
  Feature ranked list: r = []
  repeat
    Restrict training set to good feature indices
    Optimize hyperparameters of linear and RBF kernel SVM classifier
    Train the classifiers
    Compute the weight vector
    Compute the weight magnitude as ranking criterion
    Find the feature with smallest ranking criterion
    Update feature ranked list
    Eliminate the feature with smallest ranking criterion
    Predict the test set with the RBF kernel classifier
  until s = []
end for
Output: feature ranked list r
```

After SVM-RFE, we computed classification measures for feature j; accuracy ACC_j as the percentage of trials that were correctly classified, sensitivity SEN_j as the percentage of trials that were correctly classified as MCI-C, and specificity SPC_j as the percentage of trials that were correctly classified as MCI-NC. The number of features that provided the best accuracy in the SVM-RFE procedure was used as the number of features selected after SVM-RFE. As a result of SVM-RFE, we obtained a $77 \times m$ matrix L (Fig. 2), where m is the number of features of each data set. Each row of the matrix L corresponds to the feature ranked list r for the ith LOOCV iteration. The feature ranked list r is a $1 \times j$ matrix of the features ordered by relevance. The first element of the feature ranked list r had the index of the most relevant feature. More specifically, $L(i, j)$ refers to the feature number of the rank j of the ith LOOCV iteration. To obtain a final ranking of features, we first converted the matrix L to the RFE rank matrix R according to the equation $R(i, L(i, j)) = j$. We then converted the resulting RFE rank matrix R to the RFE rank score matrix S according to the following equation:

$$S(i,j) = 0 \, (R(i,j) > k)$$

or

$$S(i,j) = \frac{k - R(i,j) + 1}{k} (R(i,j) \leq k)$$

where $S(i, j)$ is the score for feature j of the ith LOOCV iteration ($0 \leq S \leq 1$); k is the number of selected features after SVM-RFE for the data set; and $R(i, j)$ is the rank number of feature j in the matrix R ($1 \leq R \leq m$; m is the number of features of the data set). Then we

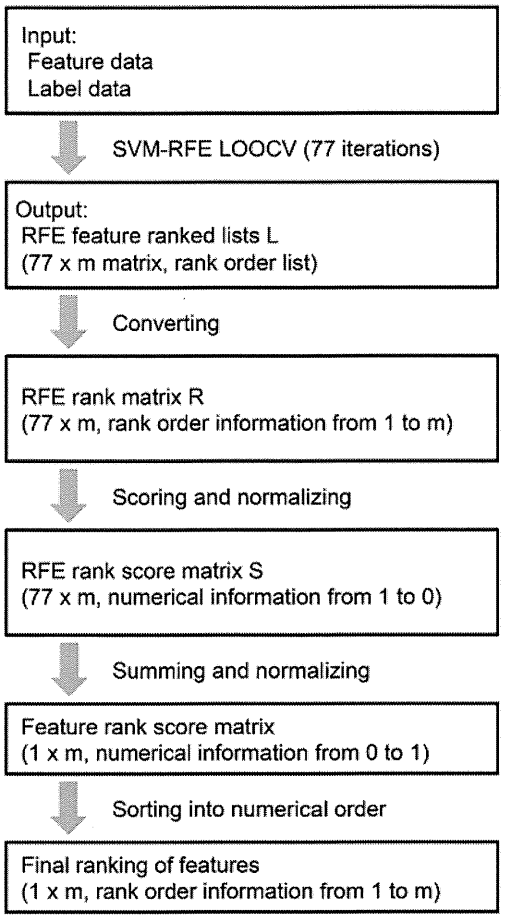

Fig. 2. Schematic representation of how to obtain a final ranking of features after SVM-RFE. In the figure, *m* refers to the number of features of a data set.

computed the sum of each column of the RFE rank score matrix *S* and normalized the resulting matrix between 0 and 1 to obtain a $1 \times m$ feature rank score matrix. We sorted these feature rank scores into numerical order to obtain a final selection ranking of features after SVM-RFE for each atlas data set (Supplementary Table 3).

2.7. Statistical analysis

In order to investigate whether the classification accuracies were significantly different from one another, we applied leave-one-out cross validation a hundred times using different atlases and with features selected through the SVM-RFE procedure. Two-way ANOVA followed by Tukey's multiple comparison test was performed for statistical analysis of atlas and feature selection using the statistical software packages R version 2.15.2 (The R Foundation for Statistical Computing, http://www.r-project.org/). To examine the behavior of the classifiers, we generated receiver operating characteristics (ROC) curves and computed areas under the curve (AUC) and 95% confidence intervals (CI) using the pROC package for R (Robin et al., 2011). CIs for AUCs were computed with DeLong's method. Pairwise comparisons of ROC curves were performed using DeLong's test implemented in the pROC package. LOOCV was also used to test these final classifiers.

3. Results

3.1. VBM analysis

Fig. 3 shows the result of VBM analysis. We found a significant cluster of GM density reduction in MCI-C compared with MCI-NC. The 2391 mm^3 cluster was located in the parahippocampal gyrus and hippocampus on the left side (peak voxel at MNI coordinate −26, −42, −9). The reverse contrast (MCI-NC < MCI-C) showed no significant regions of GM loss.

3.2. Features selected with SVM-RFE

Fig. 4 illustrates the RFE rank score matrices *S* from three brain atlases. The vertical axis of the matrix represents a subject number, i.e., each step of the LOOCV procedure. The horizontal axis represents the number of features in each atlas. The top-ranked feature (the feature that was selected last during the SVM-RFE procedure) having a score of 1 was colored in white. The score of the features that were not selected was 0 and colored in black. For example, in the map from the AAL, for the left hippocampus, feature number 37 was the most often selected during the LOOCV procedure. As can be seen from Fig. 4, "hot" regions that were often selected and "cold" regions that were rarely selected almost tidily line up vertically, suggesting that similar regions were selected through each step of the LOOCV procedure.

Fig. 5 lists the regions that were selected with the SVM-RFE procedure, which revealed the highest performance in the three brain atlases. In AAL, 20 regions out of 116 were selected, 20 out of 82 in BA, and 37 out of 56 in LPBA40. The left hippocampus was in the highest rank in AAL, which is consistent with the results of the VBM analysis. In BA, the left parahippocampal region was ranked first. In LPBA40, the left parahippocampal gyrus was ranked second following the left inferior occipital gyrus.

Fig. 6 illustrates selected region maps with the SVM-RFE procedure overlaid to representative structural MR images. The regions with the highest rank are colored in white and the lowest rank are colored in black. The results of AAL and BA were similar, e.g., the left hippocampal region was the most often selected. In contrast, more regions that included the left hippocampal region were often selected in LPBA40.

3.3. SVM classification combined with SVM-RFE

Fig. 7 shows the plots of the classification accuracy versus the number of selected features in the dataset extracted with each brain atlas and selected based on the SVM-RFE. First, the classification accuracy differs depending on the choice of atlases. LPBA40 allowed the highest accuracy, AAL was the second, and BA was the lowest. Second, all the plots had a peak between the minimum and maximum numbers of features. The number of features at the peak, i.e., the number of features selected in the SVM-RFE procedure, was the largest in LPBA40.

Table 2 lists the sets of accuracy, sensitivity, and specificity for the classification without feature selection and with feature selection based on the SVM-RFE algorithm. As a result of the SVM-RFE-based feature selection, 20 features were selected in AAL and BA, and 37 features were selected in LPBA40. The feature selection method improved the classification accuracy in all of the atlases. The best classification performance was obtained by using LPBA40 with 37 features, giving a correct classification rate of 77.9%, a sensitivity of 76.9%, and a specificity of 78.9%. AAL with 20 features distinguished MCI-C from MCI-NC with 71.4% accuracy, 69.2% sensitivity, and 73.7% specificity. BA with 20 features reached 67.5% accuracy, 64.1% sensitivity, and 71.1% specificity.

Fig. 8 demonstrates classification accuracies obtained with features extracted using different atlases (left) and features further selected through the SVM-RFE procedure (right). Note that the accuracies shown in Fig. 8 were obtained with the fixed set of 37 features that we chose based on the ranking after SVM-RFE,